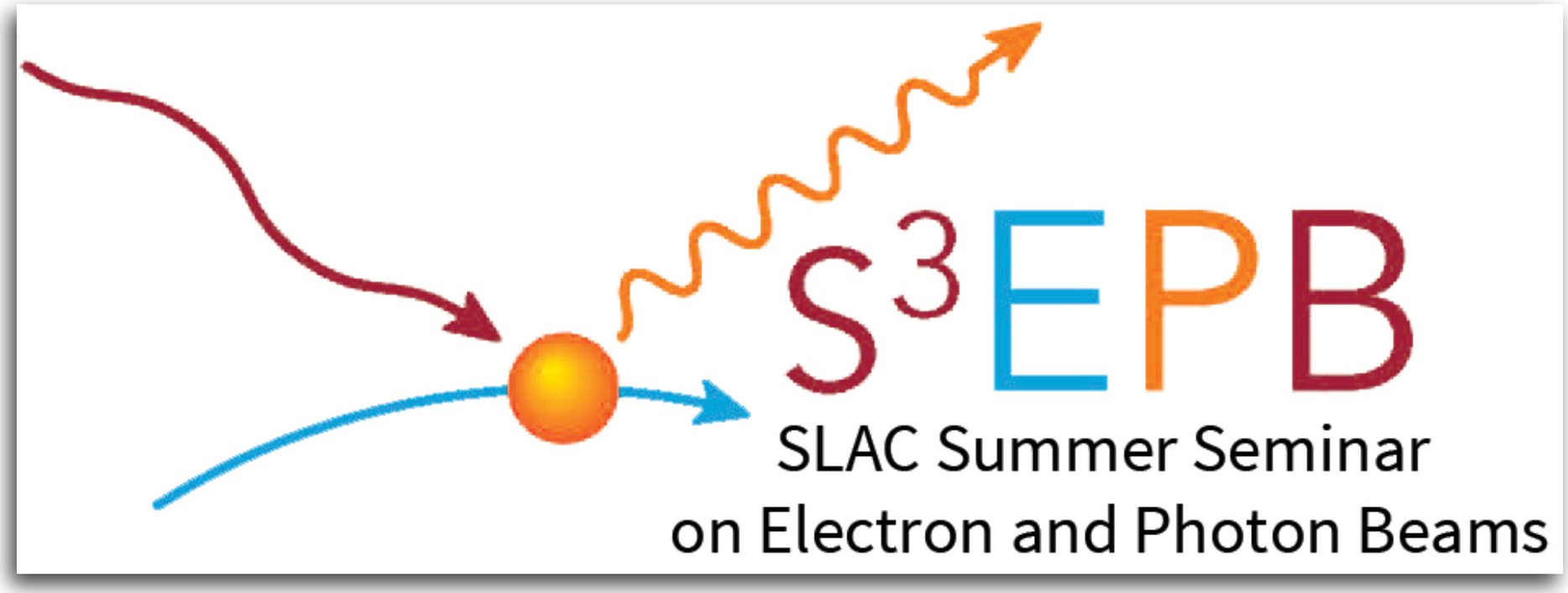

Advanced FEL Concepts

E. Hemsing
SLAC

August 3-7, 2015

Outline

- FEL Basics
  - Characteristics of FEL Radiation
- Challenges and Desirables
- Techniques (NOT exhaustive)
  - Beam shaping
  - Seeding
  - Slippage shaping
- Summary

Characteristics of FELs

- Invented by John Madey in the 1970s.
- Tunable, high power radiation 10 orders of magnitude brighter than storage ring based synchrotron light sources
- Electrons interact with the radiation field in vacuum.
- Unlike conventional lasers restricted to fixed transitions between atomic energy levels, FELs use unbound electrons and have no such limitation on their output wavelength.
- Broad frequency tunability over ~ 8 orders of magnitude
- No thermal lensing, birefringence or heat dissipation issues.
- Radiation is essentially diffraction limited, with a low angular divergence and narrow bandwidth.

Basics of FELs: 1D Model

Operating principle:

- Relativisitic electron beam travels through magnetic undulator that makes it wiggle and radiate.
- Radiation also acts back on the beam to rearrange the phase space, generating an energy modulation that grows and turns into a density modulation via the *FEL instability*.
- The radiation grows exponentially, taking energy from the e-beam and increasing the energy spread.
- The process saturates when the energy spread covers the FEL bandwidth and e-beam falls out of resonance.

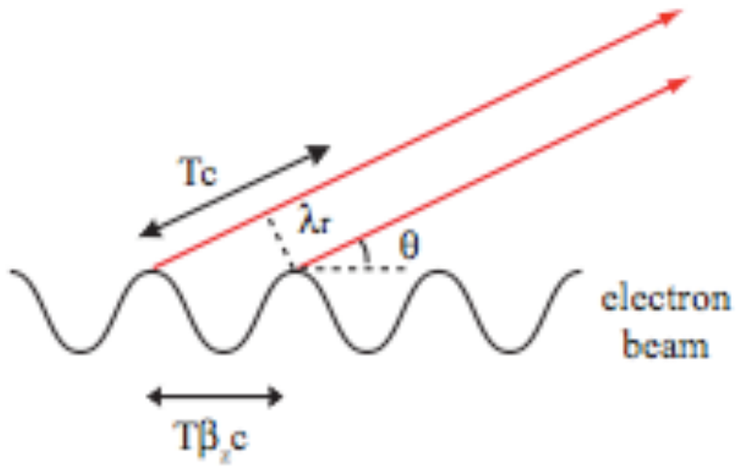

Basics of FELs: 1D Model

The rate of energy transfer between the radiation and electron is

$$\frac{d\mathcal{E}}{dt} = e\mathbf{E}\cdot\mathbf{v} \tag{1.4}$$

Now consider a horizontally polarized simple plane wave at frequency $\omega = kc$;

$$E_x = E_0 \sin k(z - ct) \tag{1.5}$$

Combining Eqs. (1.3),(1.4), and (1.5), the change in energy of the particle along the undulator length is

$$\frac{d\gamma}{dz} = \frac{-eKE_0}{\gamma mc^2}\sin(k_u z)\sin[k(z - ct(z))]. \tag{1.6}$$

Let us define the co-moving coordinate $s = z - c\bar{\beta}_z t(z)$ where $\bar{\beta}_z = 1 - (1 + K^2/2)/2\gamma^2$ is the average longitudinal velocity obtained from averaging $\beta_z = \sqrt{1 - \frac{1}{\gamma^2} - \beta_x^2}$ over each undulator period and using $\beta_x = dx/dz$ with Eq. (1.3).

Basics of FELs: 1D Model

The energy change is typically small compared to the resonant energy γ_r, so we define $\eta = (\gamma - \gamma_r)/\gamma_r$. We finally obtain two non-linear pendulum equations for the evolution of the electron:

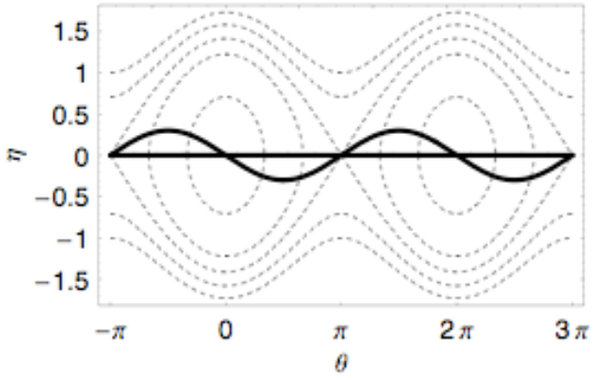

$$\frac{d\eta}{dz} = \frac{eK\mathcal{J}}{2\gamma mc^2}(\tilde{E}e^{i\theta} + \tilde{E}^* e^{-i\theta})$$
$$\frac{d\theta}{dz} = 2k_u\eta \tag{1.11}$$

Finally, in high-gain FELs, the field also grows along the undulator due to the development of microbunching in the beam. A simple but lengthy analysis shows that, from Maxwell's equations the 1D field evolution is given by

$$\frac{d\tilde{E}}{dz} = -\frac{eK\mathcal{J}}{2\gamma^2 mc^2}\langle e^{i\theta}\rangle. \tag{1.12}$$

where $\langle e^{i\theta}\rangle = b$, the bunching factor.

Basics of FELs: 1D Model

It is convenient to introduce ρ, known as the Pierce parameter, or simply the FEL parameter:

$$\rho = \left(\frac{K^2 \mathcal{J}^2 k_p^2}{32 k_u^2} \right)^{1/3} \tag{1.13}$$

where $k_p c$ is the longitudinal plasma frequency. The FEL equations can then be written in scaled form as

$$\frac{d\bar{\eta}}{d\bar{z}} = \bar{a} e^{i\theta} + \bar{a}^* e^{-i\theta}, \qquad \frac{d\theta}{d\bar{z}} = \bar{\eta}, \qquad \frac{d\bar{a}}{d\bar{z}} = -b \tag{1.14}$$

with $\bar{\eta} = \eta/\rho$, $\bar{z} = 2k_u \rho z$,and $\bar{a} = \frac{eK\mathcal{J}\tilde{E}}{2k_u \rho^2 \gamma^2 mc^2}$.
The solution for the power of the field $\langle aa^* \rangle$ along the undulator has an exponential term that grows like $e^{\sqrt{3}\bar{z}}$. The power gain length is then $L_g = \frac{1}{2\sqrt{3}k_u \rho}$.

High Gain FEL Growth and Scaling

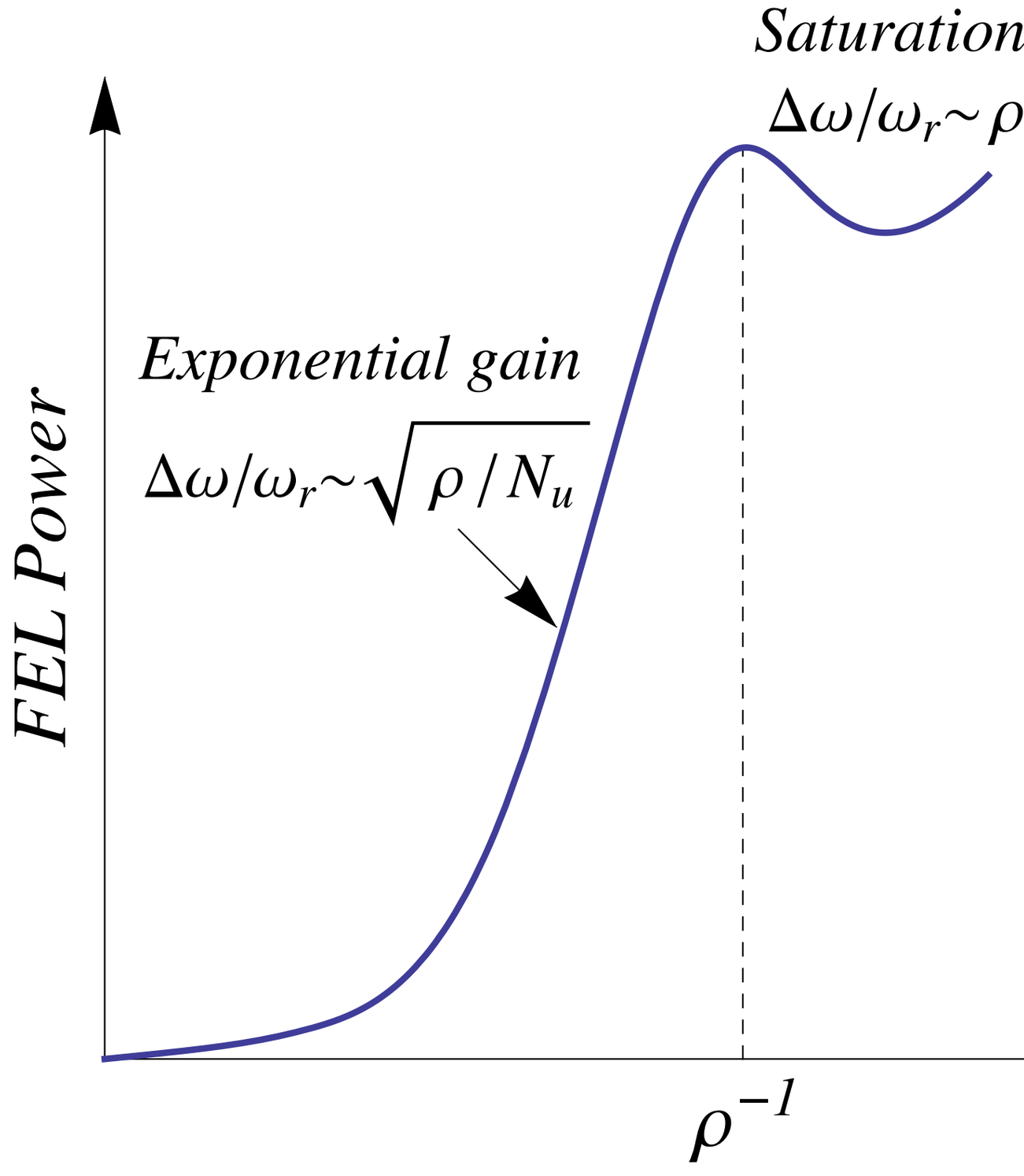

Saturation length

$$L_s \sim \lambda_u/\rho$$

Saturation power

$$P_s \sim \rho P_b = \rho \mathcal{E} I_0/e$$

Evolution of FEL and electron beam during lasing

Radiation power along undulator

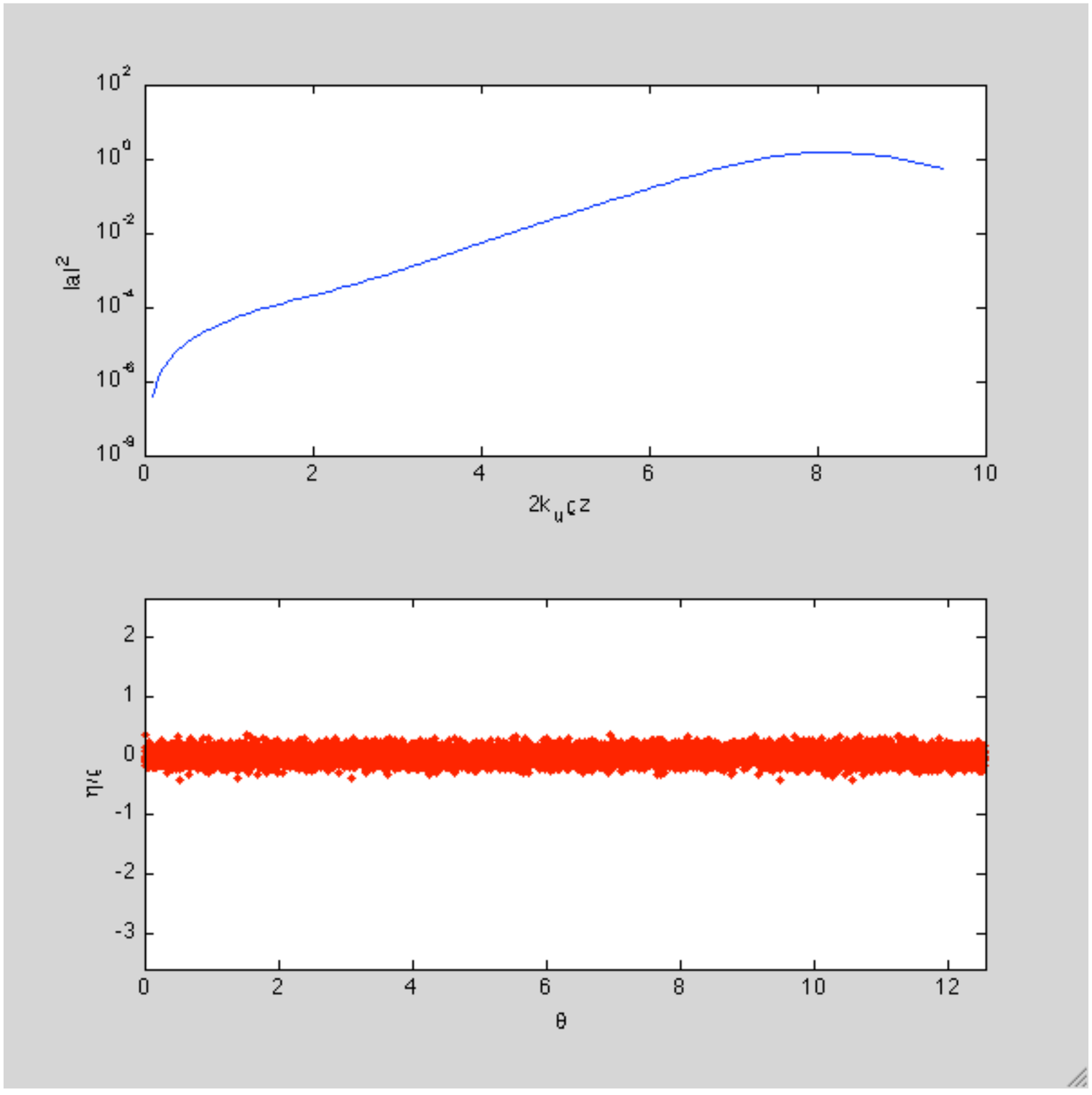

e-beam phase space

Evolution of SASE FEL (starting from noise)

Radiation power along undulator

e-beam phase space

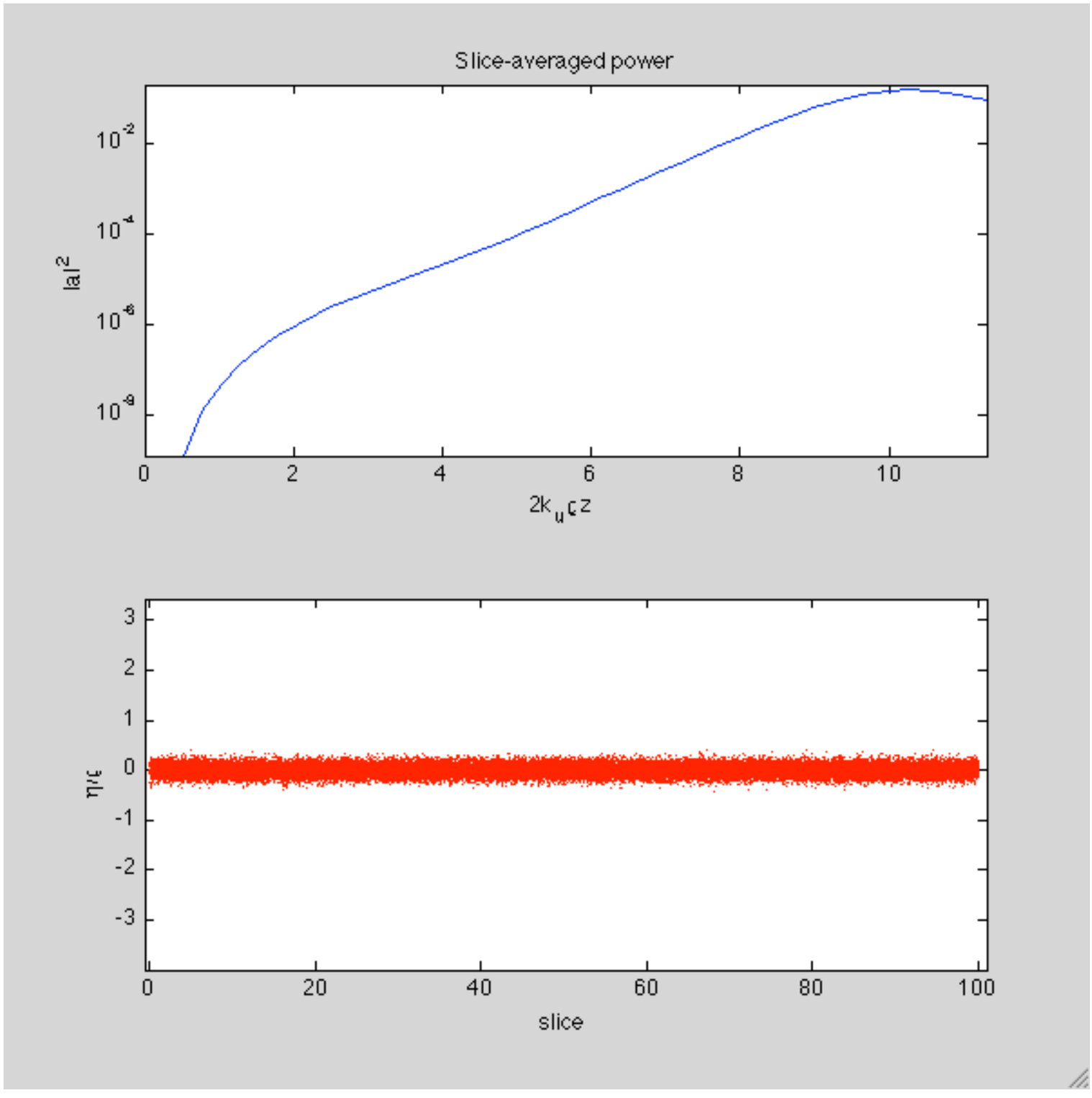

SASE FEL Output pulse

At saturation

time

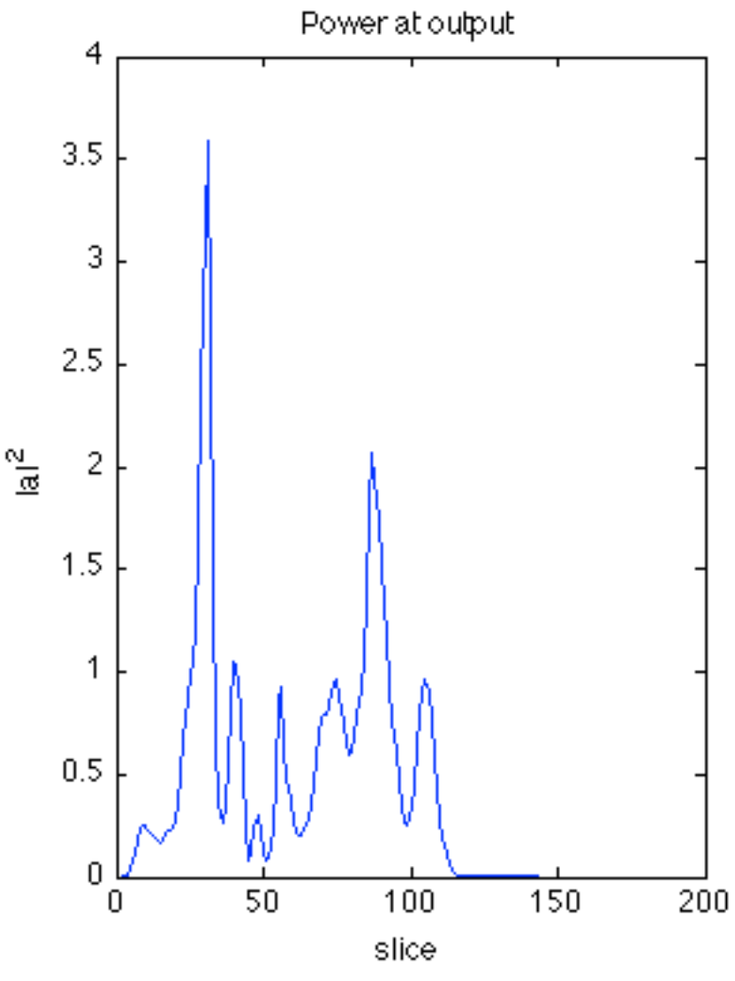

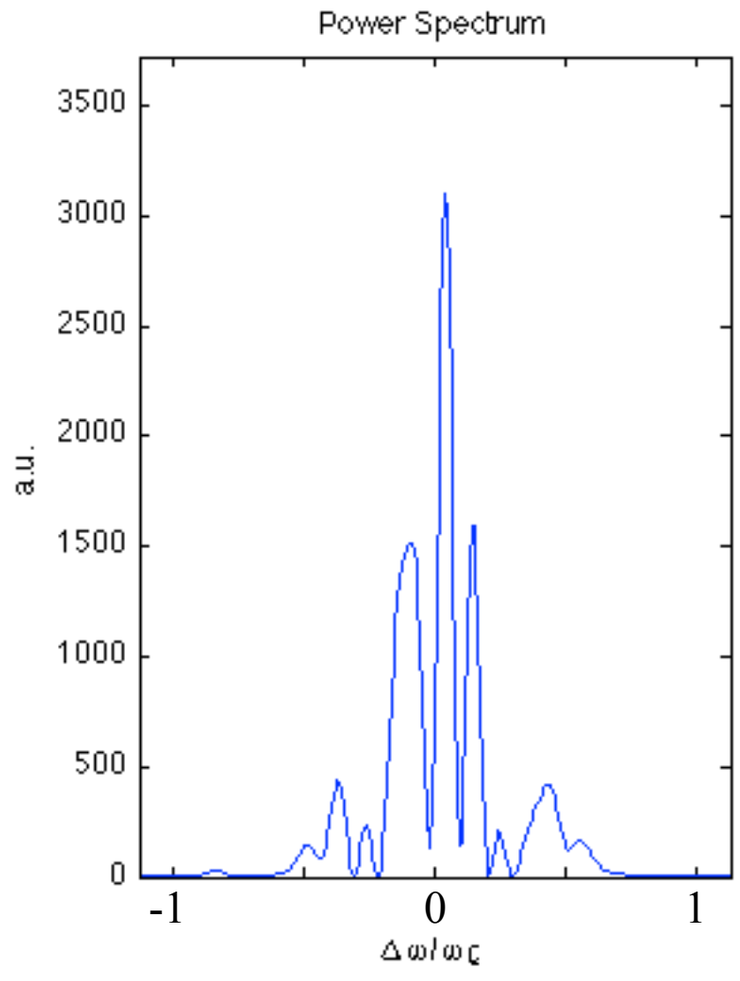

spectrum

Multiple spikes

Basics of FELs: 1D Model–Temporal Characteristics

- Self-amplified spontaneous emission (SASE) FELs start from random shot noise in the beam.
- In 1-D the initial shot noise bunching factor is $b_{\rm sn} \sim \sqrt{1/N_c}$ where $N_c = I\lambda_r/ec\rho$ is the number of electrons in the length λ_r/ρ.
- Shot noise has a broad bandwidth corresponding to short correlation length.
- Resonance maintained as electrons slip backward a distance λ_r each undulator period λ_u.
- After a gain length, the EM wave slips through the electron beam one cooperation length $l_c = \lambda_r/4\pi\sqrt{3}\rho$
- The temporal coherence length at saturation in a SASE FEL is $l_{\rm coh} \simeq \lambda_r/\rho\sqrt{2\pi}$, so the number of temporal spikes in the SASE emission $\simeq \sigma_s/l_{\rm coh}$ can be $\gg 1$.
- Statistical, large fluctuations shot to shot with bandwidth much larger than the FT limit defined by σ_s.

Challenges in free-electron lasers

1: Temporal coherence.

- Most modern high-gain VUV to hard x-ray FELs operate in SASE mode to multi-gigawatt level. Despite excellent transverse coherence, SASE FELs have limited temporal coherence and exhibit large statistical fluctuations in the output power spectrum.
- Full coherence desirable.

2: Control over the x-ray pulse duration.

- Electron bunch length typically longer than the cooperation length (tens of fs) as limited by the electron bunch length. But resolution of electron motion in atoms needs x-ray pulses down to attoseconds (10^{-18} s).
- Tunable pulse duration desirable.

Challenges in free-electron lasers

3. Ultra-high power x-ray pulses, for studies of matter in extreme conditions and imaging with "diffraction before destruction".
   - FEL power can be enhanced both by increasing the beam peak current (e.g., P_b and ρ), and undulator tapering. Laser enhancements may yield coherent x-rays up to 5 TW through current-enhanced electron microbunches and temporal shifts between the FEL radiation and the micro-bunch train.
   - Ultra-high power

4. Radiation shaping
   - Mode-locked x-ray FELs with single radiation pulses with equally spaced sharp spectral lines useful for single-shot resonant inelastic x-ray scattering spectroscopy, time-resolved three-wave mixing, stimulated Raman scattering, etc.
   - Helical phases carrying variable photon polarization and OAM enable with new photon degrees of freedom
   - Customizable pulses desirable

Short Pulses through Beam Shaping

- Want a short FEL pulse? Make the electron beam short!
- Single spike SASE output for beams shorter than the FEL cooperation length
- Low charge
- Diminishing returns in making the beam shorter

Nuclear Instruments and Methods in Physics Research A 593 (2008) 39–44

Contents lists available at ScienceDirect

Nuclear Instruments and Methods in Physics Research A

journal homepage: www.elsevier.com/locate/nima

Generation of ultra-short, high brightness electron beams for single-spike SASE FEL operation

J.B. Rosenzweig [a,*], D. Alesini [c], G. Andonian [a], M. Boscolo [c], M. Dunning [a], L. Faillace [b,c], M. Ferrario [c], A. Fukusawa [a], L. Giannessi [e], E. Hemsing [a], G. Marcus [a], A. Marinelli [b,c], P. Musumeci [a], B. O'Shea [a], L. Palumbo [b,c], C. Pellegrini [a], V. Petrillo [d], S. Reiche [a], C. Ronsivalle [e], B. Spataro [c], C. Vaccarezza [c]

[a] UCLA Department of Physics and Astronomy, 405 Hilgard Ave., Los Angeles, CA 90095, USA

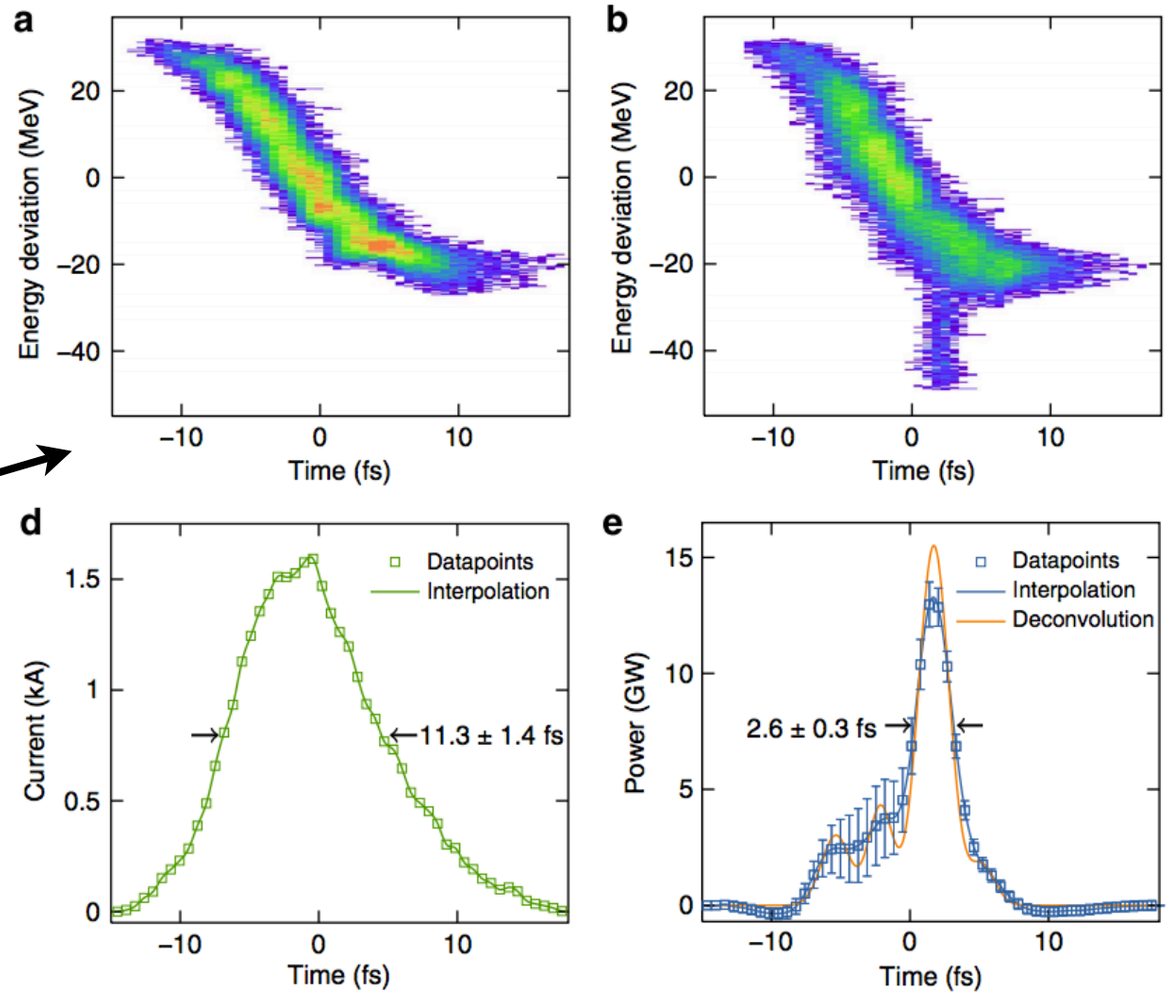

nature COMMUNICATIONS

ARTICLE

Received 6 Jan 2014 | Accepted 31 Mar 2014 | Published 30 Apr 2014

DOI: 10.1038/ncomms4762

Few-femtosecond time-resolved measurements of X-ray free-electron lasers

C. Behrens[1,2], F.-J. Decker[1], Y. Ding[1], V.A. Dolgashev[1], J. Frisch[1], Z. Huang[1], P. Krejcik[1], H. Loos[1], A. Lutman[1], T.J. Maxwell[1], J. Turner[1], J. Wang[1], M.-H. Wang[1], J. Welch[1] & J. Wu[1]

Short Pulses through Beam Shaping

- Slotted Foil aka “Emittance Spoiler”
- Only portion of beam that passes through hole retains properties suitable for lasing

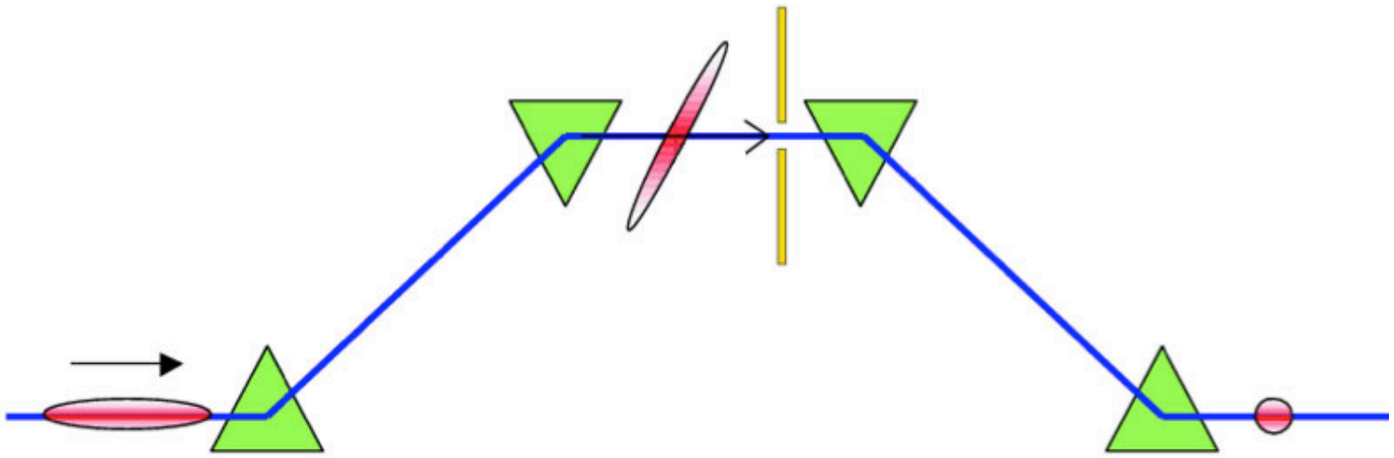

- Width of “V” determines bunch length
- Multiple short pulses with adjustable timing from double-slotted foil

Generate coherent x-ray pulses longer than cooperation length

Coherent FEL pulses can be produced if the FEL starts from a fully coherent seed that has sufficient power to dominate over the electron beam shot noise, thereby overcoming the SASE startup process.

- Self-seeding (monochromatized FEL pulse seeds downstream section)
- External laser seeding (amplify coherent EM seed: FEL amplifier)
- Prebunching (density modulation in beam seeds coherent startup)

Ex: Evolution of Seeded FEL (starting from prebunching)

Radiation power along undulator

e-beam phase space

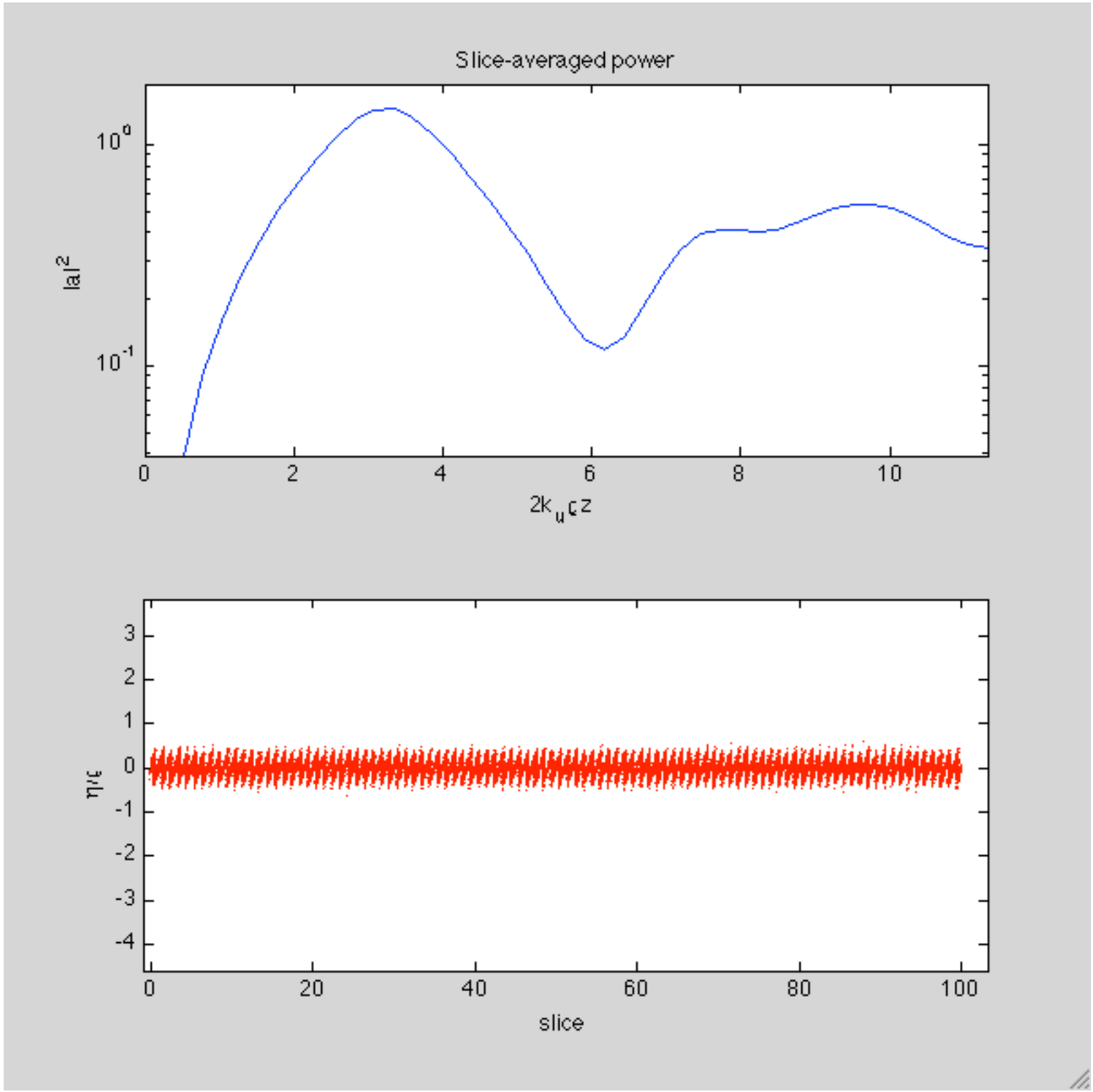

Ex. Seeded FEL Output pulse

At saturation

time

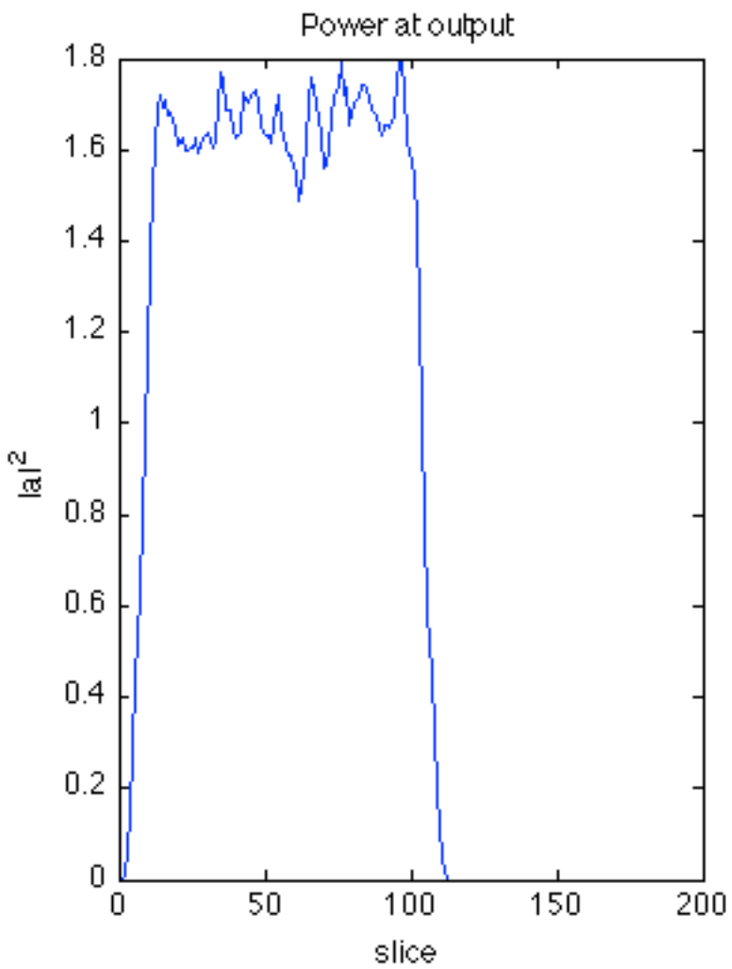

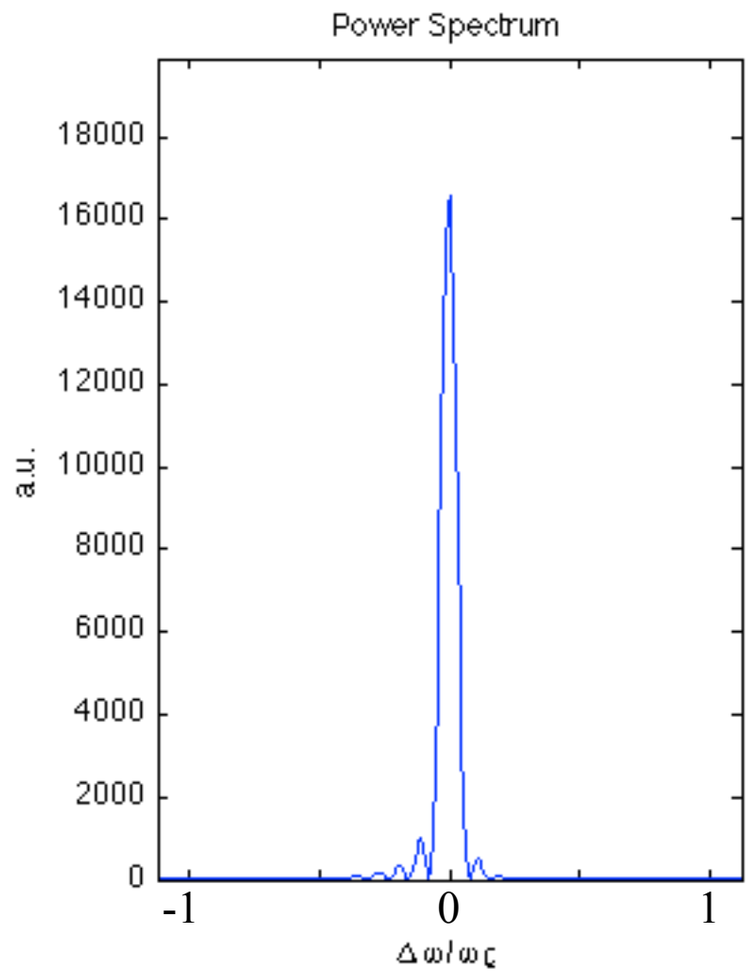

spectrum

Single spike

Self Seeding at soft x-rays

J. Feldhaus et al. / Optics Communications 140 (1997) 341–352

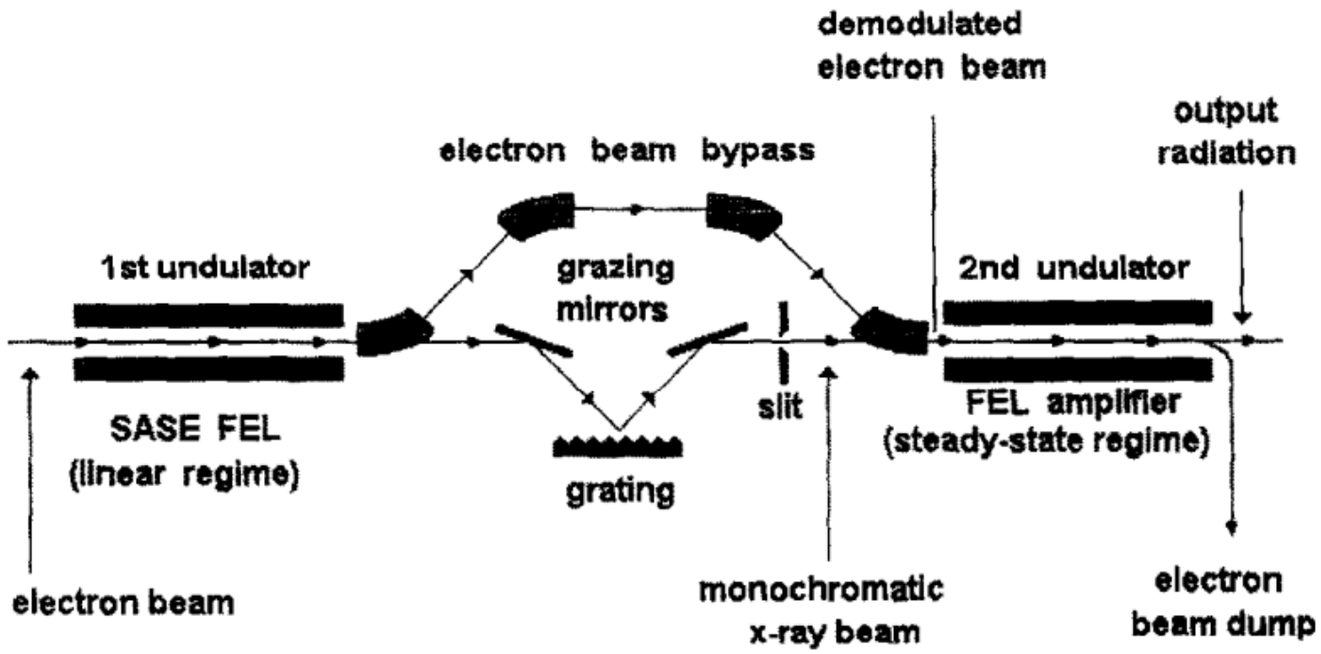

Fig. 3. The principal scheme of a single-pass two-stage SASE X-ray FEL with monochromator.

Experimental Demonstration of a Soft X-Ray Self-Seeded Free-Electron Laser

D. Ratner,[1,*] R. Abela,[2] J. Amann,[1] C. Behrens,[1] D. Bohler,[1] G. Bouchard,[1] C. Bostedt,[1] M. Boyes,[1] K. Chow,[3] D. Cocco,[1] F. J. Decker,[1] Y. Ding,[1] C. Eckman,[1] P. Emma,[1] D. Fairley,[1] Y. Feng,[1] C. Field,[1] U. Flechsig,[2] G. Gassner,[1] J. Hastings,[1] P. Heimann,[1] Z. Huang,[1] N. Kelez,[1] J. Krzywinski,[1] H. Loos,[1] A. Lutman,[1] A. Marinelli,[1] G. Marcus,[1] T. Maxwell,[1] P. Montanez,[1] S. Moeller,[1] D. Morton,[1] H. D. Nuhn,[1] N. Rodes,[3] W. Schlotter,[1] S. Serkez,[4] T. Stevens,[3] J. Turner,[1] D. Walz,[1]

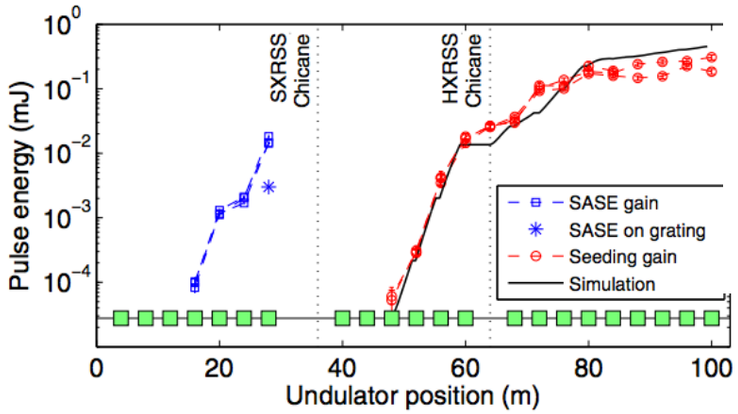

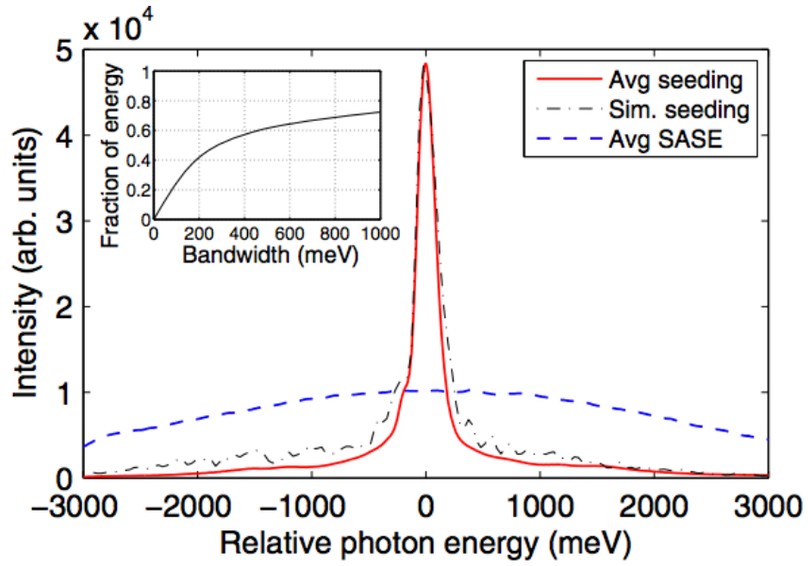

Self Seeding at hard x-rays

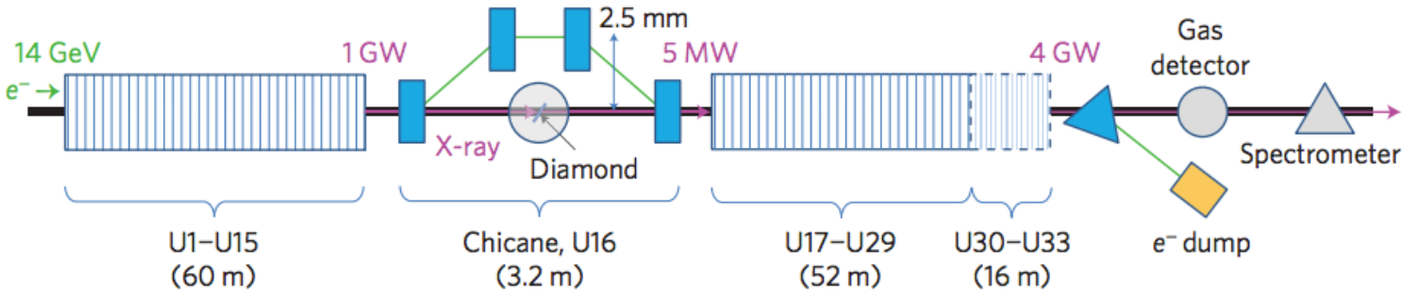

Figure 1 | Layout of the LCLS undulator with a self-seeding chicane, diamond monochromator, gas detector and hard-X-ray spectrometer. The chicane is greatly exaggerated in scale. The last four LCLS undulators (U30–U33) were previously modified as second-harmonic afterburners[15] and were not used in this experiment.

Crystal monochromator instead of grating to reduce required e-beam delay

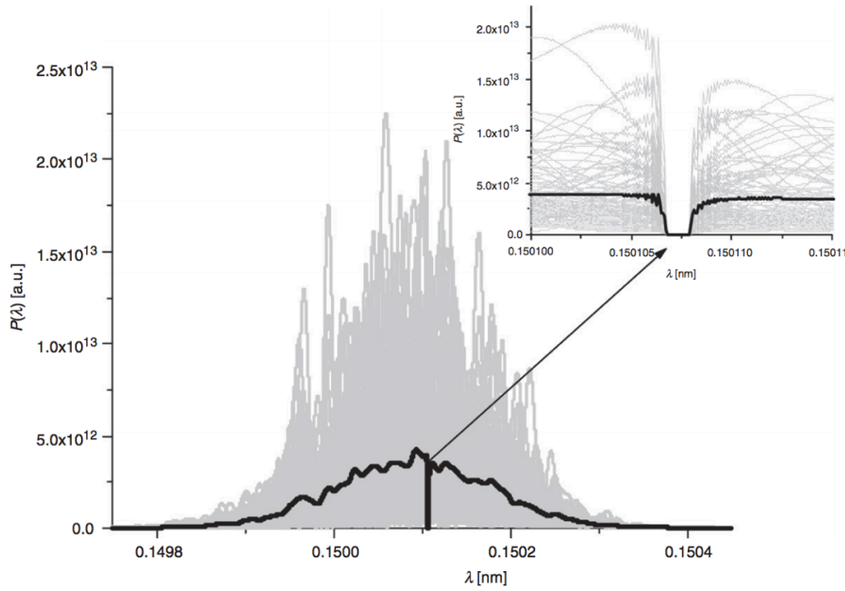

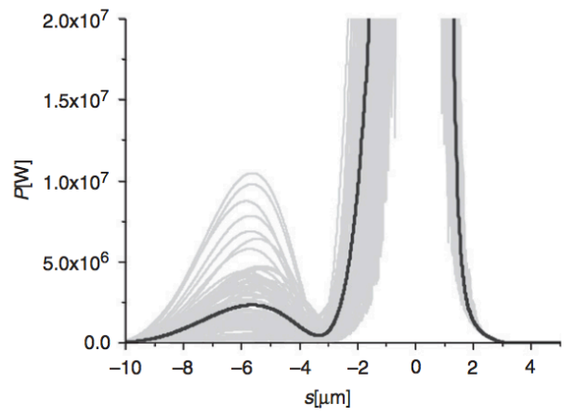

Figure 10. Feasibility study for the LCLS. Power distribution after the diamond crystal. The monochromatic tail due to the transmission through the bandstop filter is now evident on the left of the figure. Gray lines refer to single shot realizations, the black line refers to the average over 100 realizations.

Gianluca Geloni , Vitali Kocharyan & Evgeni Saldin (2011) A novel self-seeding scheme for hard X-ray FELs, Journal of Modern Optics, 58:16, 1391-1403,

nature photonics

ARTICLES

PUBLISHED ONLINE: 12 AUGUST 2012 | DOI: 10.1038/NPHOTON.2012.180

Demonstration of self-seeding in a hard-X-ray free-electron laser

J. Amann[1], W. Berg[2], V. Blank[3], F.-J. Decker[1], Y. Ding[1], P. Emma[4]*, Y. Feng[1], J. Frisch[1], D. Fritz[1], J. Hastings[1], Z. Huang[1], J. Krzywinski[1], R. Lindberg[2], H. Loos[1], A. Lutman[1], H.-D. Nuhn[1], D. Ratner[1], J. Rzepiela[1], D. Shu[2], Yu. Shvyd'ko[2], S. Spampinati[1], S. Stoupin[2], S. Terentyev[3], E. Trakhtenberg[2], D. Walz[1], J. Welch[1], J. Wu[1], A. Zholents[2] and D. Zhu[1]

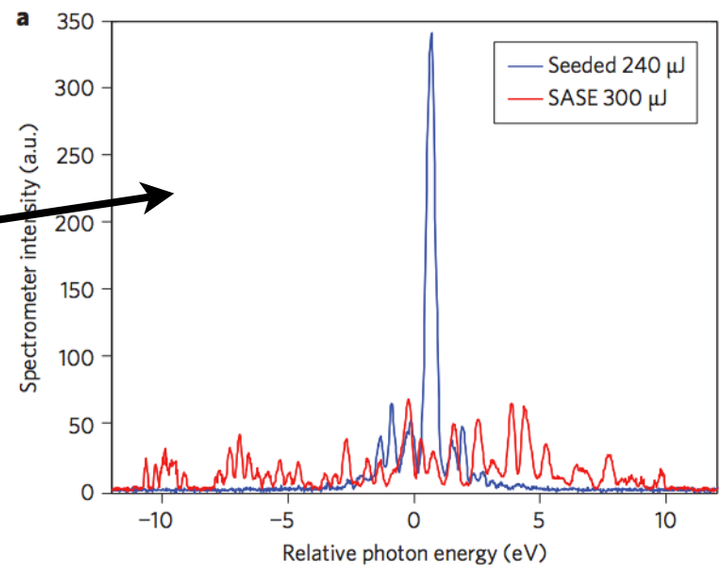

Electron beam manipulations using lasers to create bunching

Combination of one modulator and one chicane

We consider the standard setup shown below which is used to imprint optical density modulations on relativistic beams. This setup is typically used for the coherent harmonic generation (CHG) and for high-gain harmonic generation (HGHG) in Free Electron Lasers (FELs)

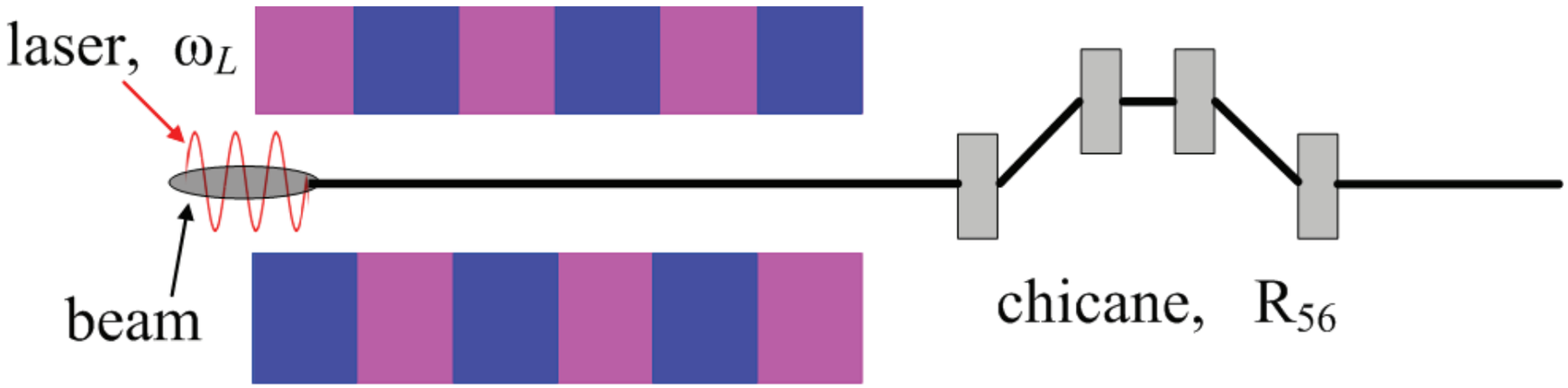

Figure : The beam energy is modulated in an undulator due to the interaction with a laser beam. The beam then passes through a dispersion section to form a density modulation.

Combination of one modulator and one chicane - Mathematical description

We assume an initial Gaussian beam energy distribution with an average energy $\mathcal{E}_0$ and the rms energy spread $\sigma_\mathcal{E}$, and use the variable $p = (\mathcal{E} - \mathcal{E}_0)/\sigma_\mathcal{E}$ for the dimensionless energy deviation of a particle. The initial longitudinal phase space distribution can then be written as

$$f(p) = \frac{N_0}{\sqrt{2\pi}} e^{-p^2/2} \tag{1.1}$$

where N_0 is the number of electrons per unit length of the beam. After passage through the undulator, the beam energy is modulated with the amplitude $\Delta\mathcal{E}$, so that the final dimensionless energy deviation p' is related to the initial one p by the equation

$$p' = p + A\sin(k_L s), \tag{1.2}$$

where $A = \Delta\mathcal{E}/\sigma_\mathcal{E}$, and s is the longitudinal coordinate in the beam.

Combination of one modulator and one chicane - Mathematical description

The distribution function after the interaction with the laser becomes

$$f(\zeta, p') = \frac{N_0}{\sqrt{2\pi}} \exp\left[-(p' - A\sin\zeta)^2/2\right] \tag{1.3}$$

where we now use the dimensionless variable $\zeta = k_L s$.

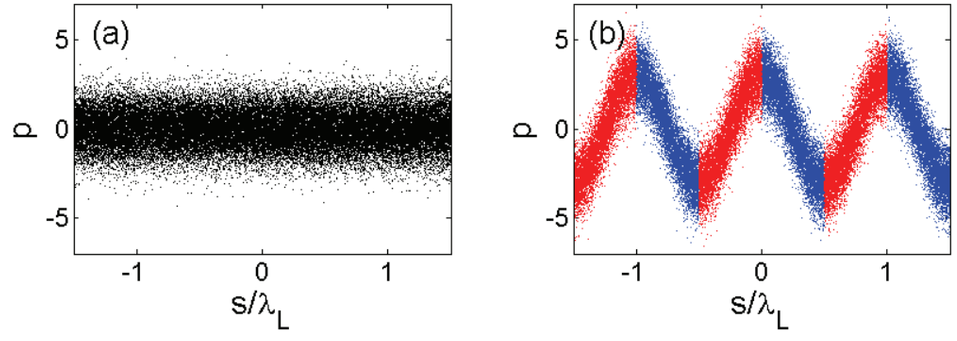

Figure : Evolution of the longitudinal phase space in the HGHG scheme with $A = 3$. (a) before the modulator; (b) after the modulator

The sinusoidal energy modulation generates regions of chirp with alternating sign that can then be compressed or decompressed by dispersive transport elements.

Combination of one modulator and one chicane - Mathematical description

The beam then passes through the dispersion section with dispersive strength R_{56}, which converts the longitudinal coordinate s into s',

$$s' = s + R_{56} p' \sigma_{\mathcal{E}} / \mathcal{E}_0 \tag{1.4}$$

The distribution function is then,

$$f(\zeta', p') = \frac{N_0}{\sqrt{2\pi}} \exp\left[-\frac{1}{2}\left(p' - A\sin(\zeta' - Bp')\right)^2\right], \tag{1.5}$$

where $B = R_{56} k_L \sigma_{\mathcal{E}} / \mathcal{E}_0$.

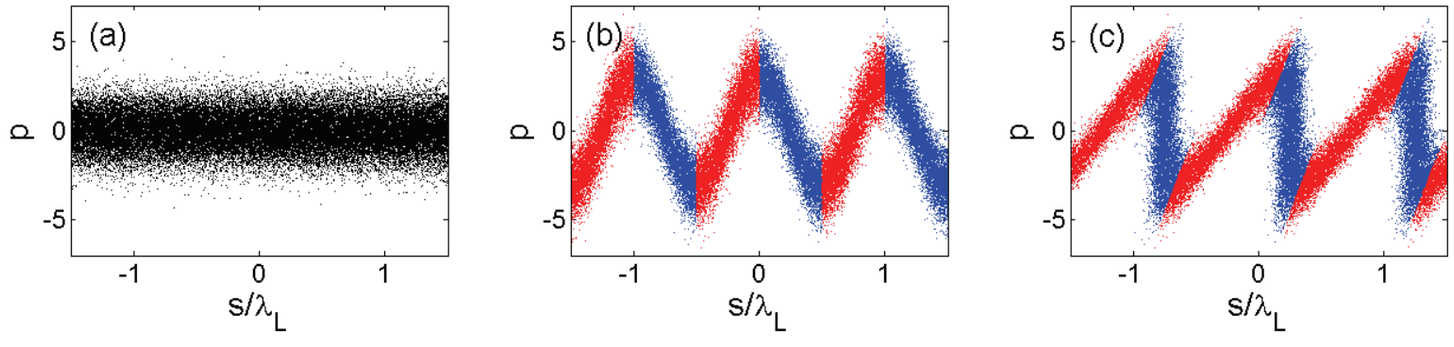

Combination of one modulator and one chicane - Mathematical description

It is convenient to describe the amplitude of the density modulations in terms of a 'bunching factor', which we define as

$$b_n = \int dp' d\zeta' f(\zeta', p') e^{-in\zeta'} \tag{1.6}$$

The integrals can be computed simply by transforming back to the original coordinates:

$$\begin{aligned} b_n &= \int dp' d\zeta f(\zeta, p') e^{-in(\zeta + Bp')} \\ &= \int dp d\zeta f(p) e^{-in(\zeta + Bp + AB \sin \zeta)} \\ &= e^{-\frac{1}{2}B^2 n^2} J_n(-ABn) \end{aligned} \tag{1.7}$$

where we have used the mathematical relation

$$e^{-ix\sin z} = \sum_{m=-\infty}^{\infty} e^{imz} J_m(-x) \tag{1.8}$$

and J_n is the Bessel function of order n.
With b_n defined above, the 1-D beam density (number of particles per unit length) N is written as a function of the final longitudinal coordinate ζ',

$$N(\zeta') = N_0 \int_{-\infty}^{\infty} dp' f(\zeta', p') \,. \tag{1.9}$$

Noting that this density is a periodic function of ζ', the bunching factors are the amplitudes of the Fourier series that describes the density modulation

$$\frac{N(\zeta')}{N_0} = 1 + \sum_{n=1}^{\infty} 2b_n \cos(n\zeta') \,. \tag{1.10}$$

Combination of one modulator and one chicane - Mathematical description

Equation (1.7) for the bunching factors indicates that by properly choosing the energy modulation amplitude A and the chicane's dispersive strength B, considerable bunching may be generated, not only at the laser wavelength but also at higher harmonics.

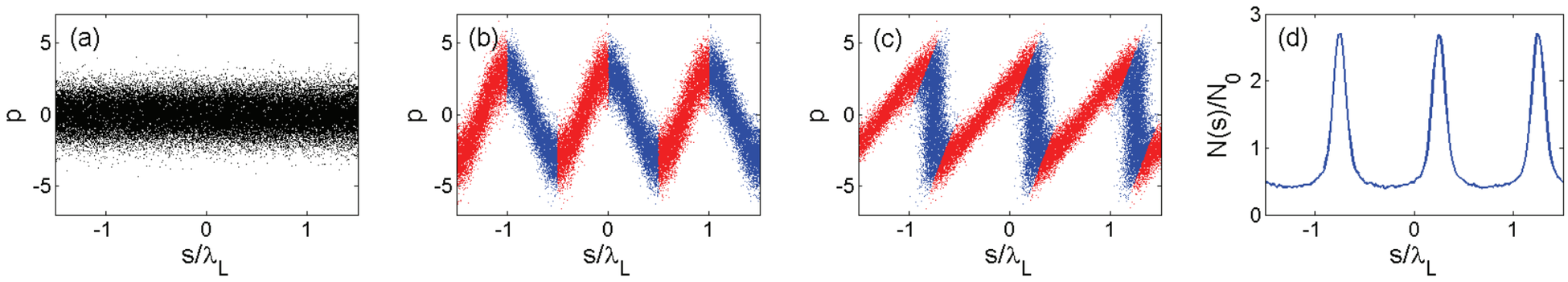

Figure : Evolution of the longitudinal phase space in the HGHG scheme with $A = 3$. (a) before the modulator; (b) after the modulator; (c) after the chicane; (d) density distribution after the chicane.

Combination of one modulator and one chicane - Mathematical description

In the limit of a large modulation amplitude, $A \gg 1$, the density (and hence current) spikes become much larger than the initial beam density (current) and the spike FWHM width Δs much shorter than the laser period. Analysis of (1.5) shows that asymptotically for large values of A,

$$\frac{N_{\max}}{N_0} \approx 1.5A^{2/3}, \qquad \Delta s \approx 0.5\frac{\lambda_L}{A}. \tag{1.11}$$

We see that when $A \gg 1$ the spikes become much narrower than the wavelength λ_L, so high harmonics are produced in the beam's current spectrum. These can be used to seed the coherent amplification of light in FELs at harmonics of the modulating laser frequency.

High Gain Harmonic Generation (HGHG) FELs

Example: FERMI FEL (Italy)

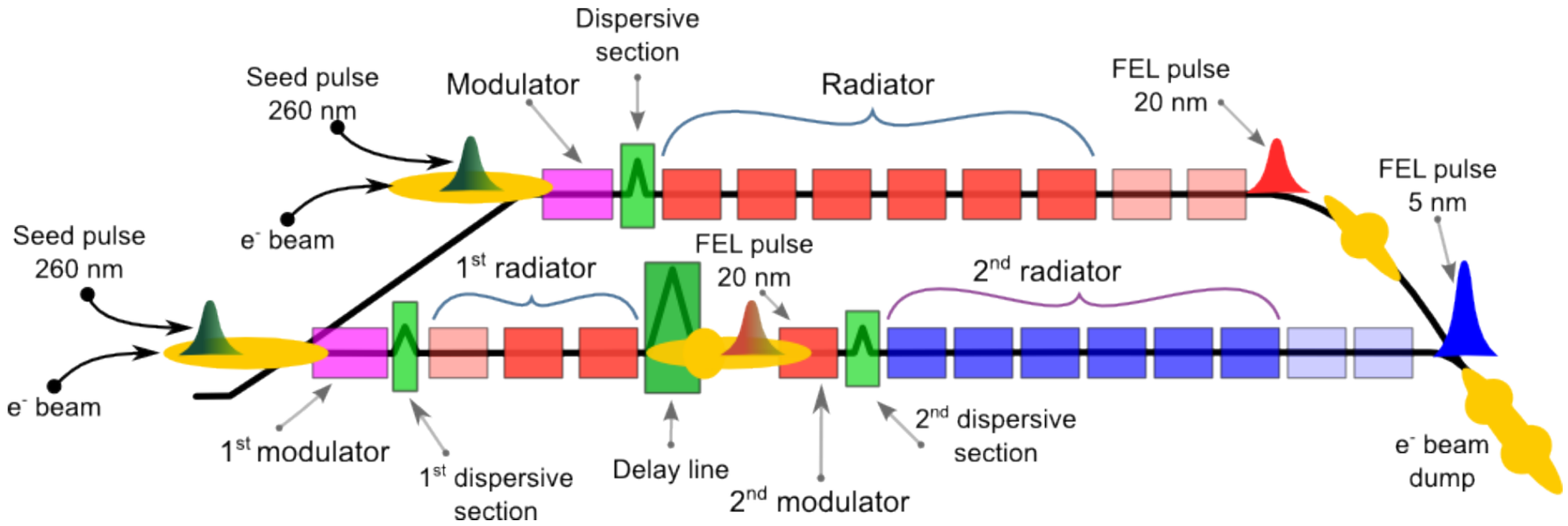

nature photonics
ARTICLES
PUBLISHED ONLINE: 23 SEPTEMBER 2012 | DOI: 10.1038/NPHOTON.2012.233

Highly coherent and stable pulses from the FERMI seeded free-electron laser in the extreme ultraviolet

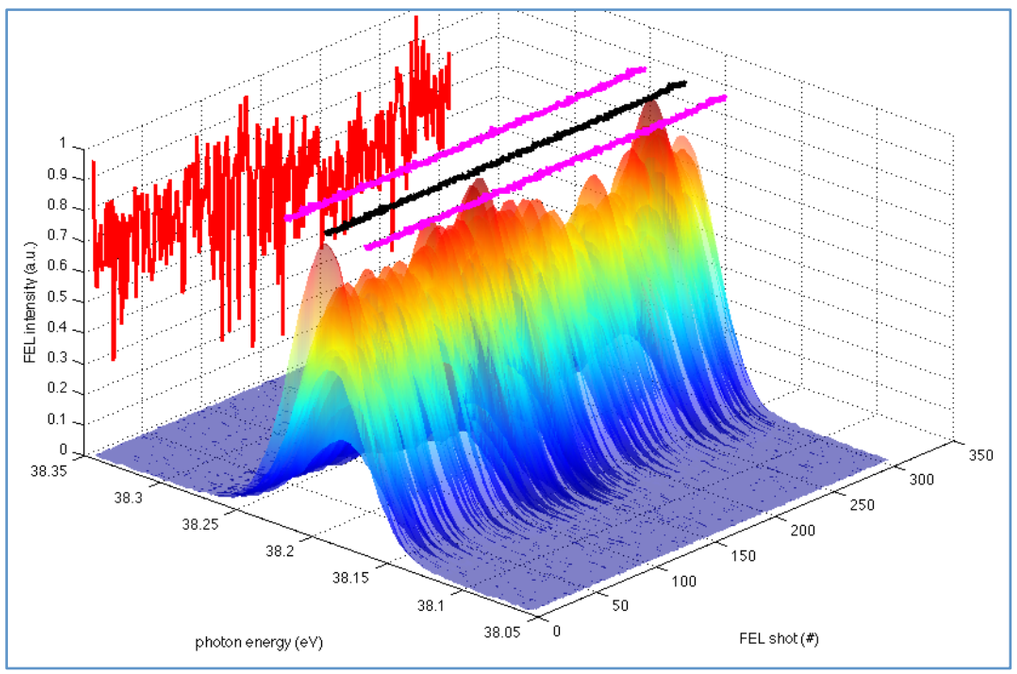

Limitations on single stage HGHG

- **Low up-frequency conversion efficiency:** $\Delta E / \sigma_E \approx n$

$\Delta E / \sigma_E = 3$

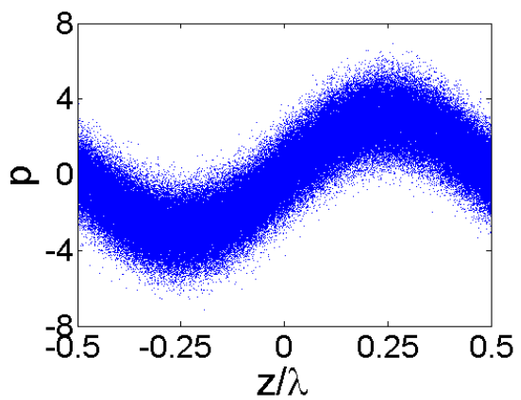

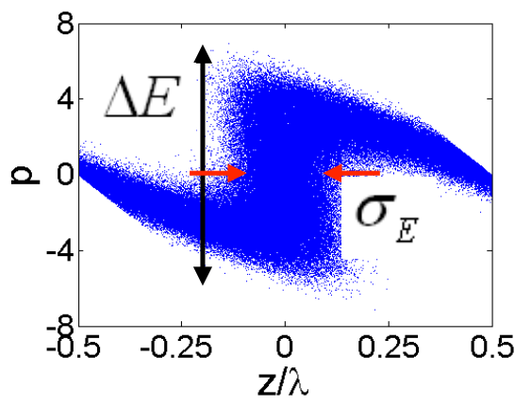

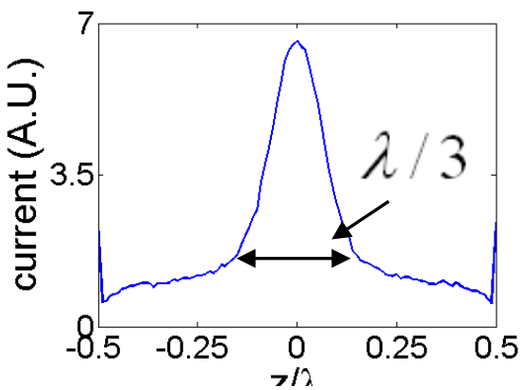

$\Delta E / \sigma_E = 10$

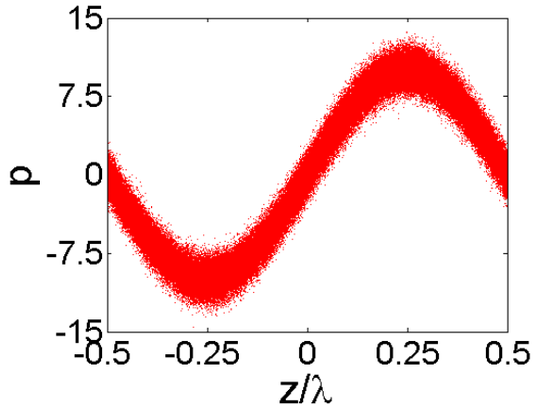

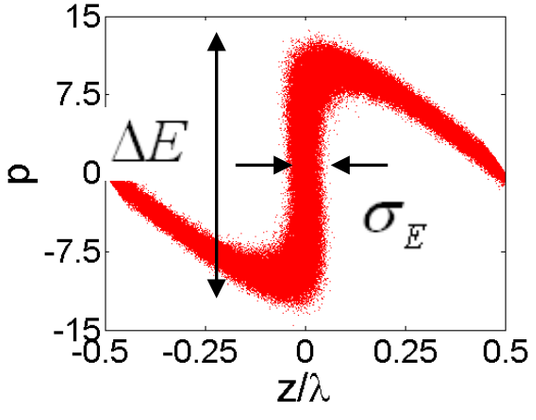

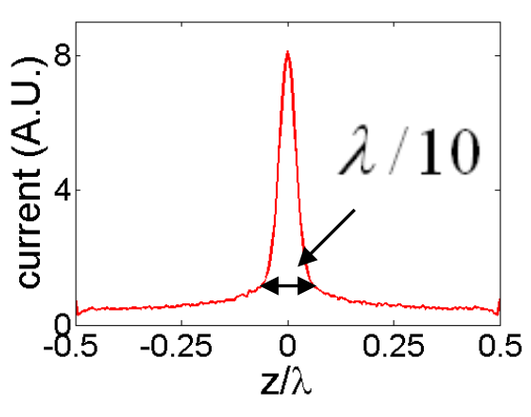

Modulator exit **Chicane exit** **Current distribution**

- **Outcome: Bunching (large ΔE) OR Gain (small ΔE)**
- **But seeded FEL wants: Bunching AND Gain**

The exponential suppression factor in

$$b_n = e^{-\frac{1}{2}B^2n^2} J_n(-ABn) \tag{1.12}$$

makes it difficult to obtain usable bunching factors for large n unless the dispersion B is also reduced to $B \sim n^{-1}$. Because the Bessel function is peaked when its argument is $\sim n$, this in turn requires an increase in the amplitude of the laser modulation to approximately $A \sim n$. Physically, this is because the longitudinal phase space area is conserved, so the $\sim n$th harmonic requires compression by the factor n, but the slice energy spread in this narrow region also increases by n. For a beam with vanishingly small energy spread, very high harmonics can be obtained since the maximal bunching factor scales as $b_n \sim n^{-1/3}$, as dictated by J_n. In reality, however, it is typically desirable to keep the induced energy spread small, so high harmonics are typically limited to values $n \lesssim 10$.

Combination of two modulators and two chicanes - Mathematical description

Consider now two modulators and two dispersion sections. This scheme was proposed under the name of Echo-Enabled Harmonic Generation (EEHG). Compared to HGHG and its variants, EEHG can produce a much higher harmonic with a relatively small energy modulation.

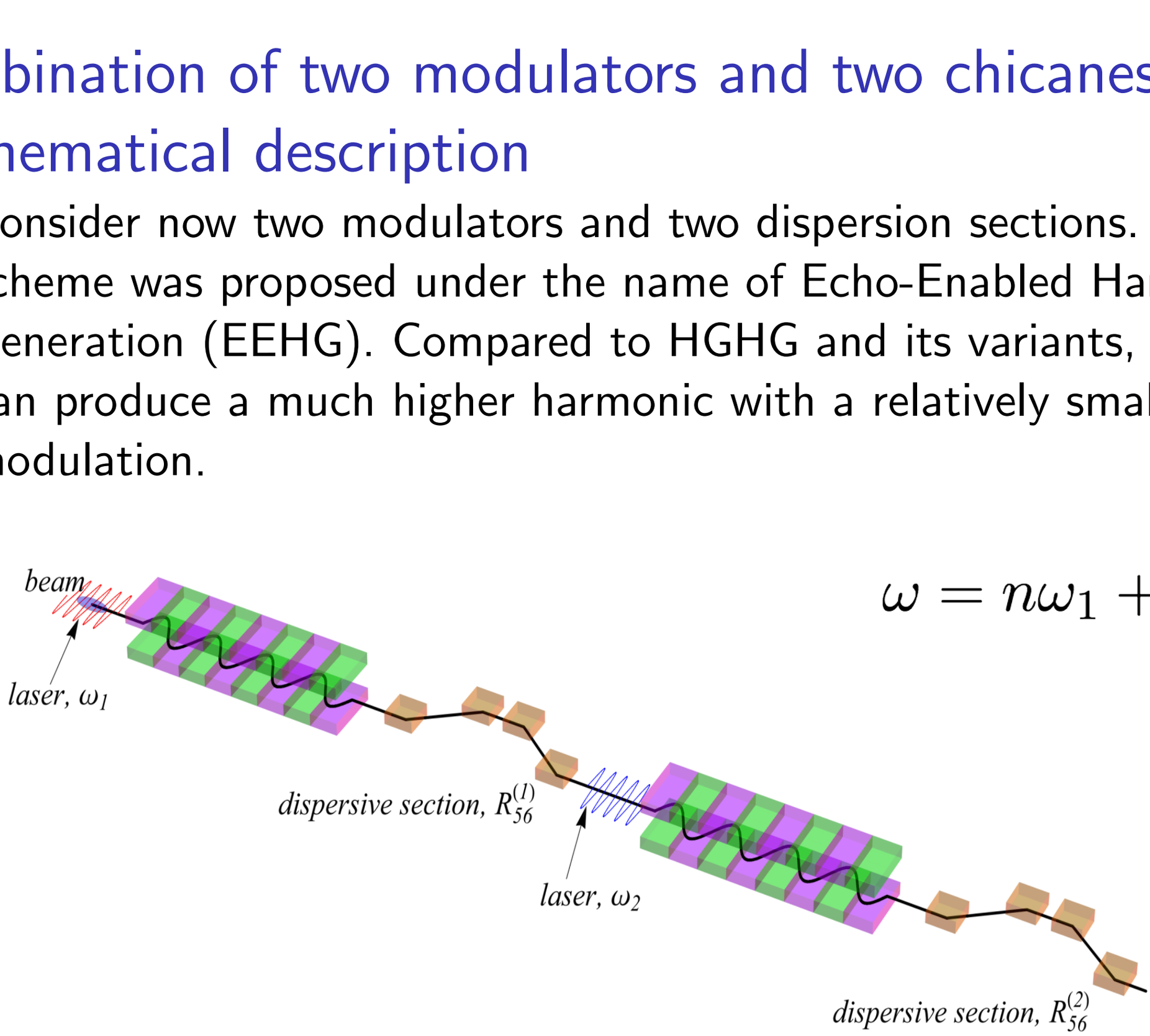

G. Stupakov, PRL 102, 074801 (2009)
D. Xiang and G. Stupakov, 12, 030702 (2009)

Combination of two modulators and two chicanes - Mathematical description

Consider now two modulators and two dispersion sections. This scheme was proposed under the name of Echo-Enabled Harmonic Generation (EEHG). Compared to HGHG and its variants, EEHG can produce a much higher harmonic with a relatively small energy modulation.

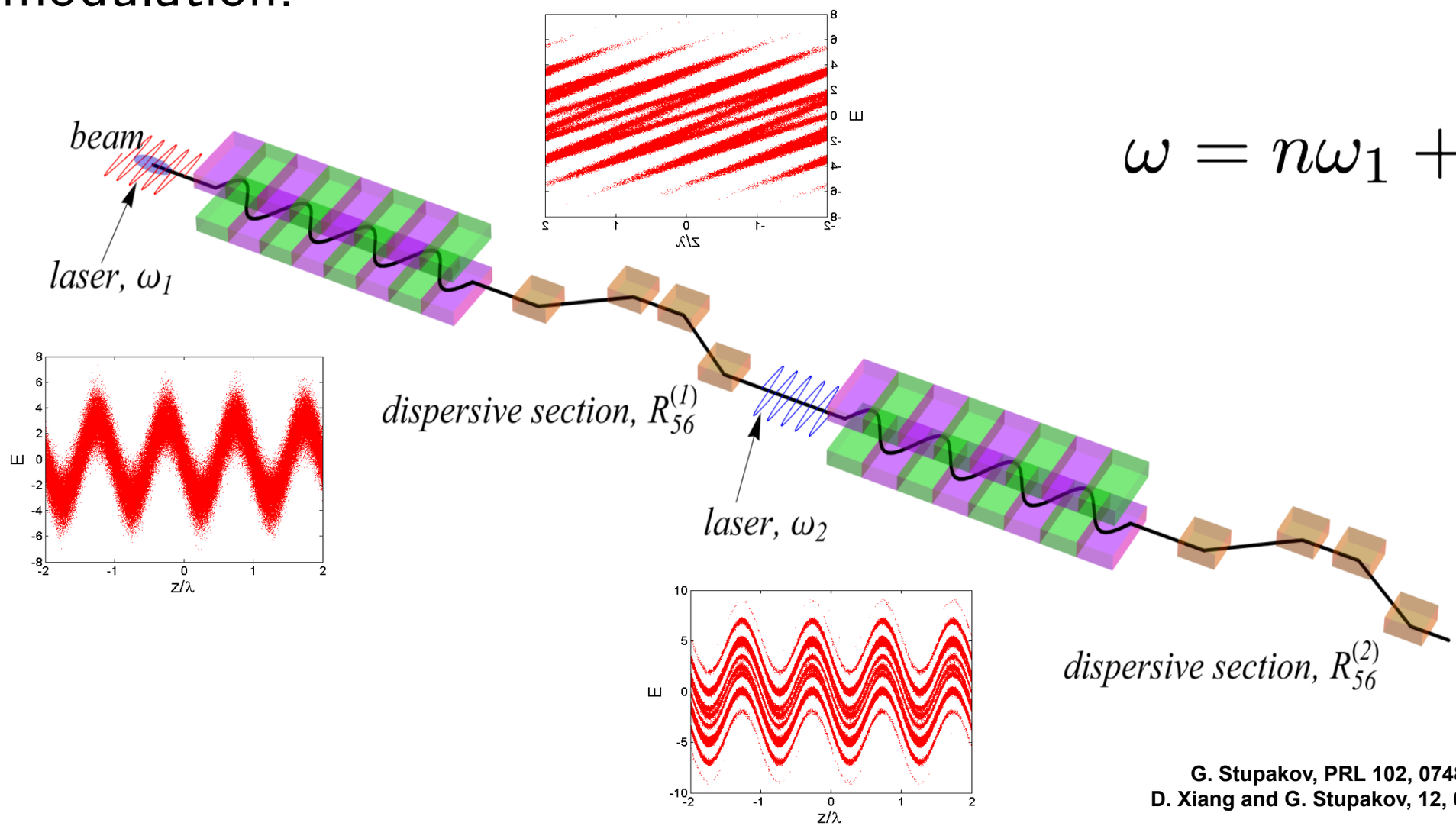

$$\omega = n\omega_1 + m\omega_2$$

G. Stupakov, PRL 102, 074801 (2009)
D. Xiang and G. Stupakov, 12, 030702 (2009)

Combination of two modulators and two chicanes - Mathematical description

Consider now two modulators and two dispersion sections. This scheme was proposed under the name of Echo-Enabled Harmonic Generation (EEHG). Compared to HGHG and its variants, EEHG can produce a much higher harmonic with a relatively small energy modulation.

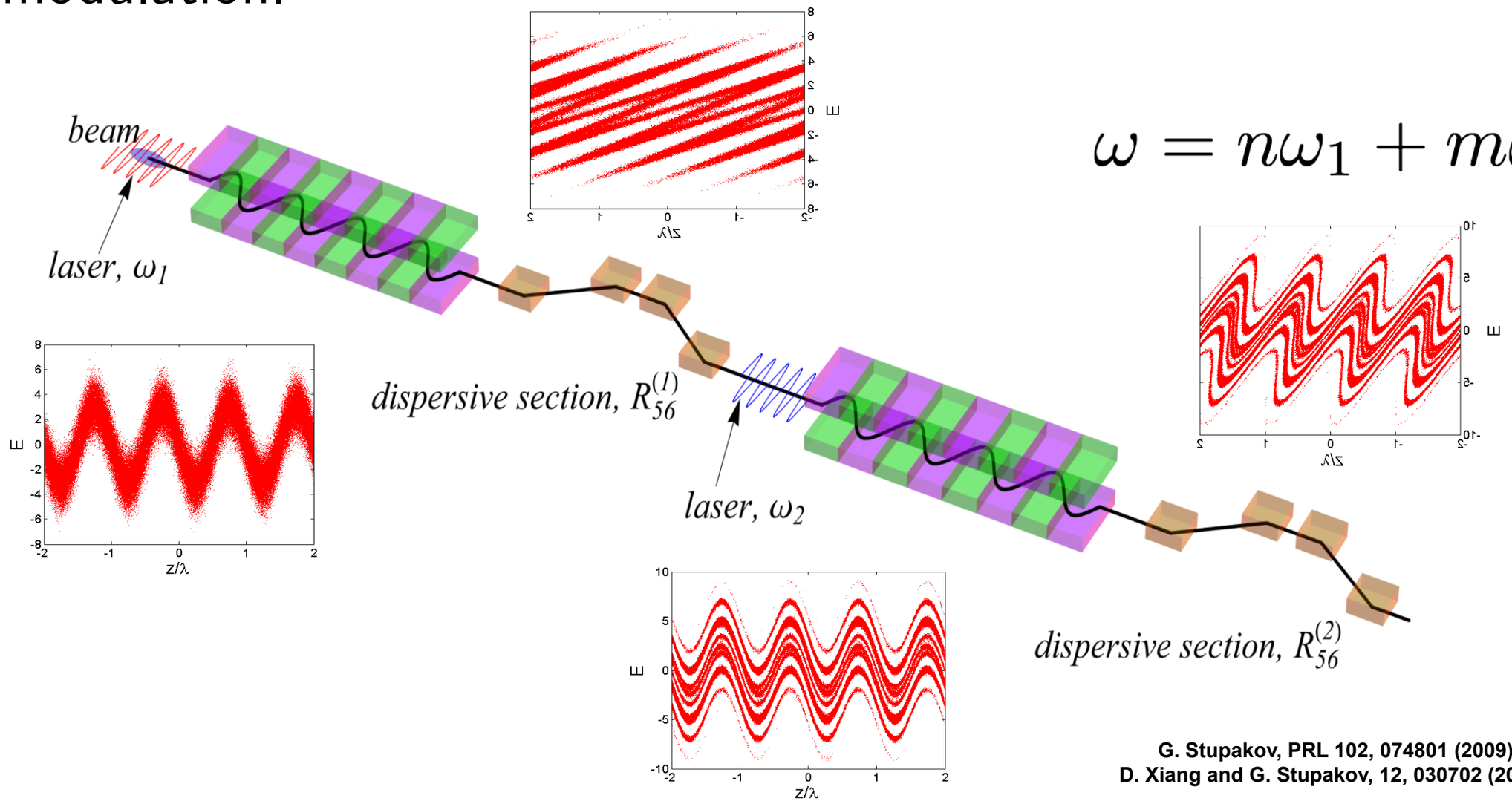

$$\omega = n\omega_1 + m\omega_2$$

G. Stupakov, PRL 102, 074801 (2009)
D. Xiang and G. Stupakov, 12, 030702 (2009)

Combination of two modulators and two chicanes - Mathematical description

The mathematical formulation of EEHG process is similar to the previous derivation. The final distribution function at the exit from the second dispersion section can be easily found by consecutively applying two more transformations to (1.2) and (1.5). The resulting final distribution function f_f is:

$$\begin{aligned} f_f(\zeta, p) = \frac{N_0}{\sqrt{2\pi}} \exp\Big[-\frac{1}{2} \big(& p - A_2 \sin(K\zeta - KB_2 p + \psi) \\ & - A_1 \sin(\zeta - (B_1 + B_2)p \\ & + A_2 B_1 \sin(K\zeta - KB_2 p + \psi)) \big)^2 \Big], \end{aligned} \tag{1.13}$$

where $\zeta = k_1 s$, $K = k_2/k_1$ with k_1 and k_2 the two laser frequencies, $A_1 = \Delta\mathcal{E}_1/\sigma_\mathcal{E}$, $A_2 = \Delta\mathcal{E}_2/\sigma_\mathcal{E}$, $B_1 = R_{56}^{(1)} k_1 \sigma_\mathcal{E}/\mathcal{E}_0$, $B_2 = R_{56}^{(2)} k_1 \sigma_\mathcal{E}/\mathcal{E}_0$, and ψ is the phase difference of the two lasers.

Combination of two modulators and two chicanes - Mathematical description

Integration of this formula over p again gives the beam density N as a function of ζ, $N(\zeta) = \int_{-\infty}^{\infty} dp f_f(\zeta, p)$. Analysis shows that at the exit from the system the beam turns out to be modulated at a combination of multiple wavenumbers of both lasers,

$$\frac{N(s)}{N_0} = \sum_{n,m=-\infty}^{\infty} 2b_{n,m} \cos[(nk_1 + mk_2)s + \psi_{n,m}], \qquad (1.14)$$

where $\psi_{n,m}$ is the modulation phase. Assuming $A_1 B_1 \gg 1$, The bunching factors $b_{n,m}$ are found to be independent of the relative phase of the two lasers and are given by

$$\begin{aligned} b_{n,m} = {} & e^{-\frac{1}{2}(nB_1+(Km+n)B_2)^2} J_m(-(Km+n)A_2B_2) \\ & \times J_n(-A_1(nB_1 + (Km+n)B_2)). \end{aligned} \qquad (1.15)$$

Combination of two modulators and two chicanes - Mathematical description

It is of practical interest to maximize the bunching factor at a high laser harmonic by varying the modulation amplitudes A_1 and A_2 and the strength of the dispersive elements B_1 and B_2. The maximum is achieved when $n = -1$ and $m > 0$, and for large values of m the maximized value of $b_{-1,m}$ is given by

$$b_{-1,m} \approx \frac{0.39}{m^{1/3}}, \tag{1.16}$$

Remarkably, and in contrast with (1.7), Eq. (1.16) does not show the exponential suppression of high harmonics; rather, in an optimized setup, the bunching factor slowly decays as $m^{-1/3}$ even for modest values of A_1 and A_2. This is the main advantage of the EEHG scheme.

Echo Enabled Harmonic Generation (EEHG) Experiments

SLAC-NLCTA

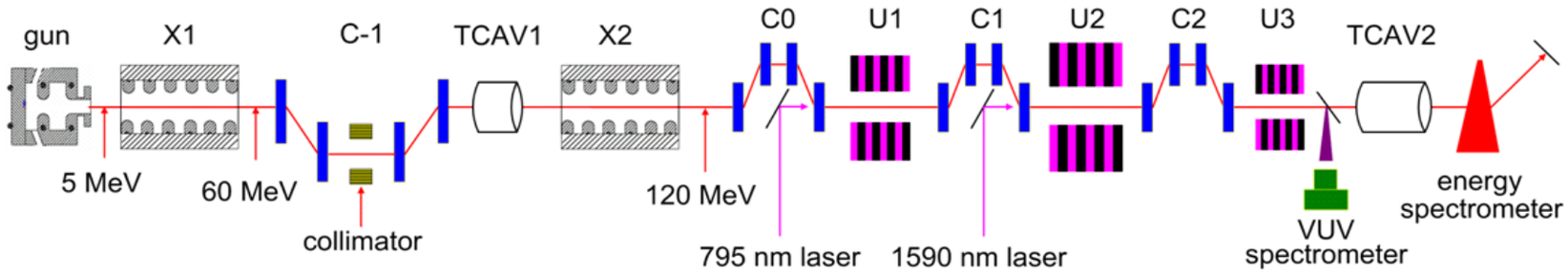

ECHO-3 (2010)

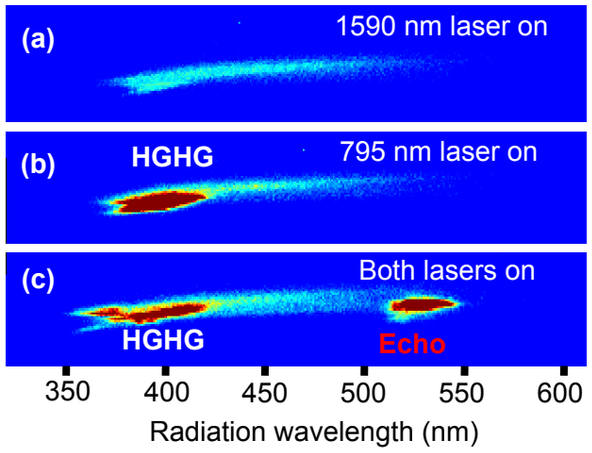

D. Xiang *et al., PRL 105, 114801* (2010)

ECHO-7 (2012)

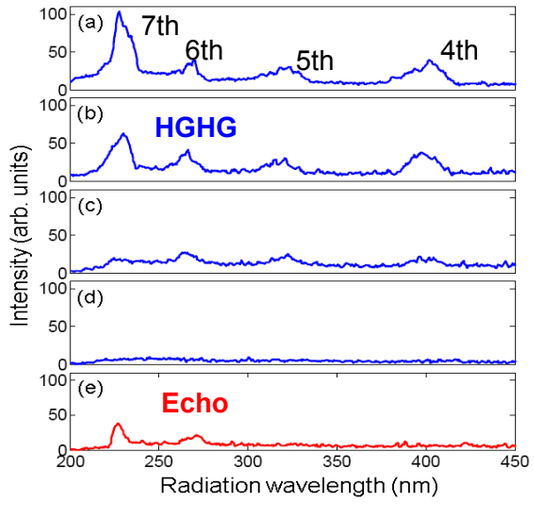

D. Xiang, et al, PRL 108, 024802 (2012).

ECHO-15 (2014)

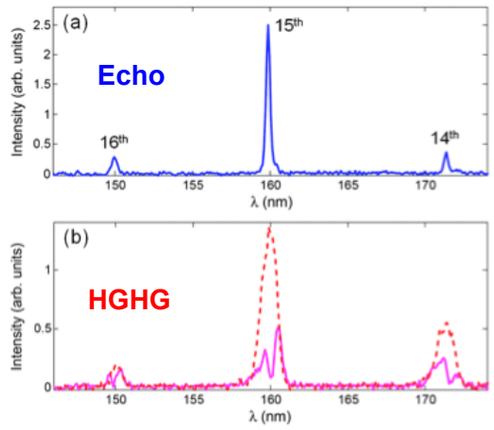

FIG. 4. Representative single-shot radiation spectrum for EEHG (a) and HGHG (b).

E. Hemsing, et al PRST-AB 17, 070702 (2014)

LETTERS
PUBLISHED ONLINE: 13 MAY 2012 | DOI: 10.1038/NPHOTON.2012.105
nature photonics

First lasing of an echo-enabled harmonic generation free-electron laser

Z. T. Zhao[1]*, D. Wang[1], J. H. Chen[1], Z. H. Chen[1], H. X. Deng[1], J. G. Ding[1], C. Feng[1], Q. Gu[1], M. M. Huang[1], T. H. Lan[1], Y. B. Leng[1], D. G. Li[1], G. Q. Lin[1], B. Liu[1], E. Prat[2], X. T. Wang[1], Z. S. Wang[1], K. R. Ye[1], L. Y. Yu[1], H. O. Zhang[1], J. Q. Zhang[1], Me. Zhang[1], Mi. Zhang[1], T. Zhang[1], S. P. Zhong[1] and Q. G. Zhou[1]

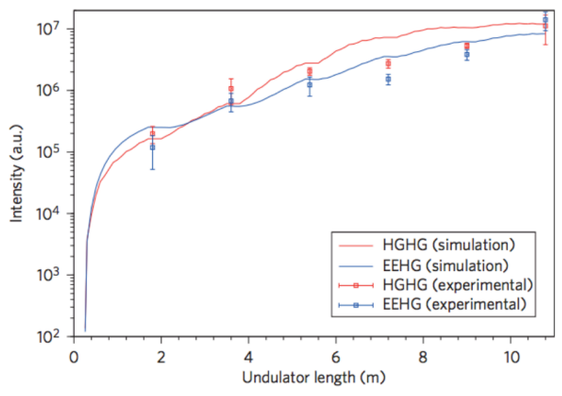

Figure 5 | Gain curves of the EEHG and HGHG FEL at SDUV-FEL. Intensity is measured with a calibrated CCD at the end of the radiator (red open squares, HGHG; blue open squares, EEHG). Error bars correspond to the peak-to-peak intensity statistics of 100 measurements. Simulation results are shown as a red line (HGHG) and a blue line (EEHG).

SDUV-FEL
(3rd harmonic 2012)

Multiple modulator-chicane modules- general form

For N successive modulator and dispersion pairs, the transformations are

$$\begin{aligned} p_N &= p_{N-1} + A_N \sin(k_N s_{N-1} + \phi_N), \\ s_N &= s_{N-1} + B_N p_N / k_1 \end{aligned} \tag{1.17}$$

where $p_N = (\mathcal{E}_N - \mathcal{E}_0)/\sigma_E$ is the scaled energy after the N^{th} modulation at the frequency k_N, $A_N = \Delta\mathcal{E}_\mathcal{N}/\sigma_\mathcal{E}$, $B_N = R_{56}^{(N)} k_1 \sigma_\mathcal{E}/\mathcal{E}_0$, ϕ_N is the laser phase, and s_N is the electron's longitudinal coordinate. The longitudinal bunching factor at the frequency k is then

$$b(k) = \langle \int e^{-iks_N} f_f(s_N, p_N) dp_N \rangle, \tag{1.18}$$

where $f_f(s_N, p_N)$ is the final e-beam distribution, and brackets denote averaging over the final coordinates,
$\langle \ldots \rangle = \lim_{L\to\infty} \frac{1}{2L} \int_{-L}^{L} \langle \ldots \rangle ds_N$

Motivation for multiple stages

- increased control of optical scale beam structure
- improved harmonic bunching
- enhanced capture efficiency for laser-based accelerators
- optical waveform synthesis

Drawbacks:

- increased complexity (more beamline components/lasers)
- stricter timing tolerances (phase error between modulator sections)

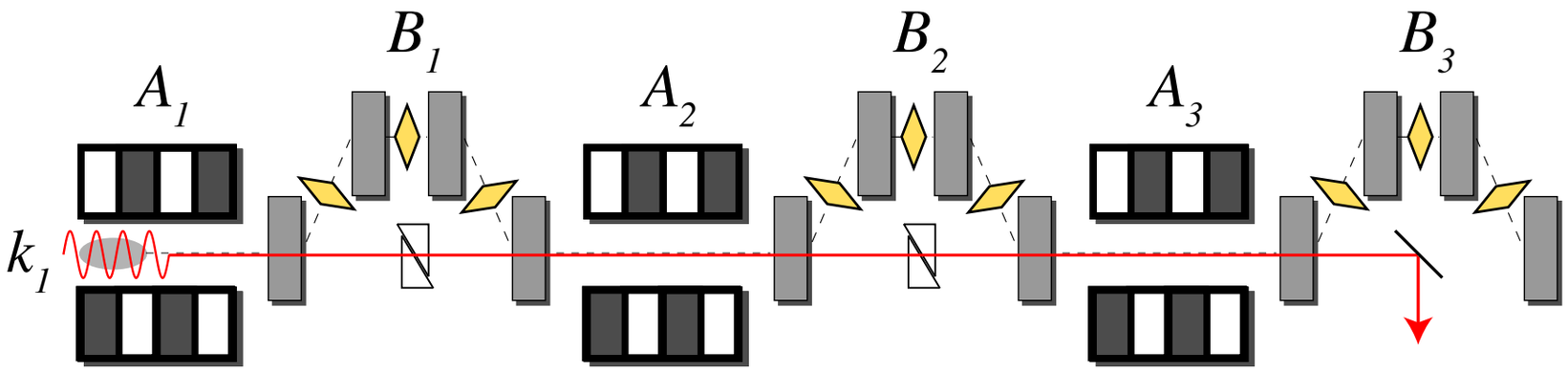

Figure : Three module example with single laser

Improving the harmonic bunching with laser harmonics

Note that the bunching factor at high harmonics in the EEHG, HGHG and CHG related schemes can be considerably increased if one can use a synthesized laser waveform that approximates a sawtooth profile. This can, in principle, be achieved by combining two or three laser harmonics with properly adjusted amplitudes and phases, or through manipulation of the beam phase space with a single harmonic as discussed later.

$$p(s) - p_0 = \frac{2A}{\pi} \sum_{h=1}^{\infty} \frac{\sin(hk_L s)}{h}. \tag{1.19}$$

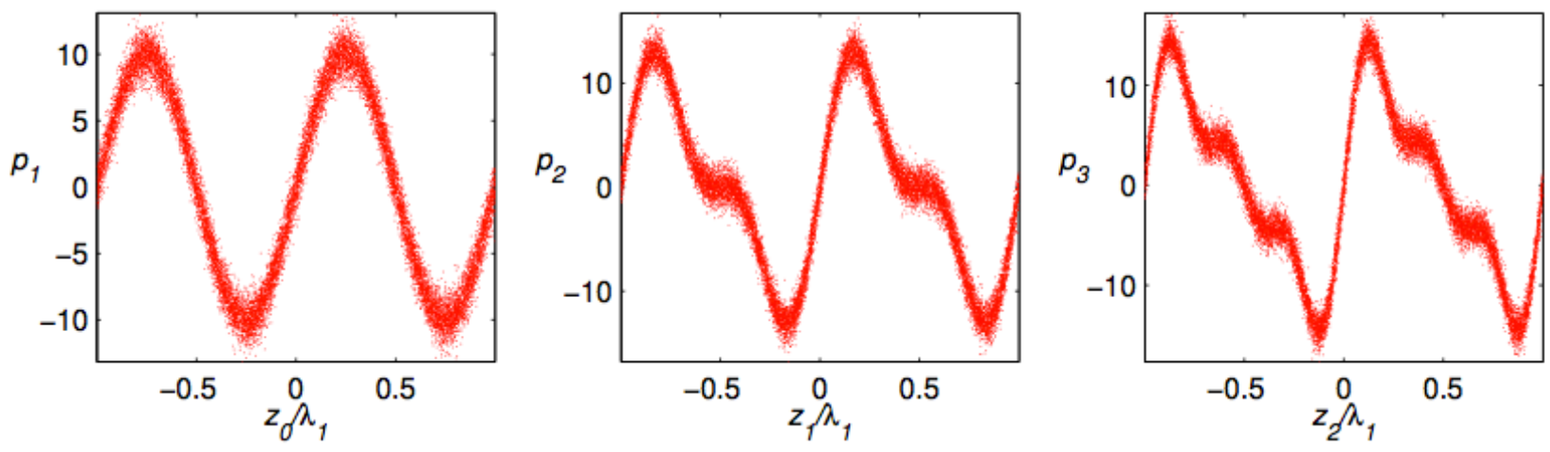

Improving the harmonic bunching with laser harmonics

In the limit of a large number of harmonic frequencies, the beam becomes separated into highly linear sawtooth regions. The bunching at the fundamental frequency can reach 100%.

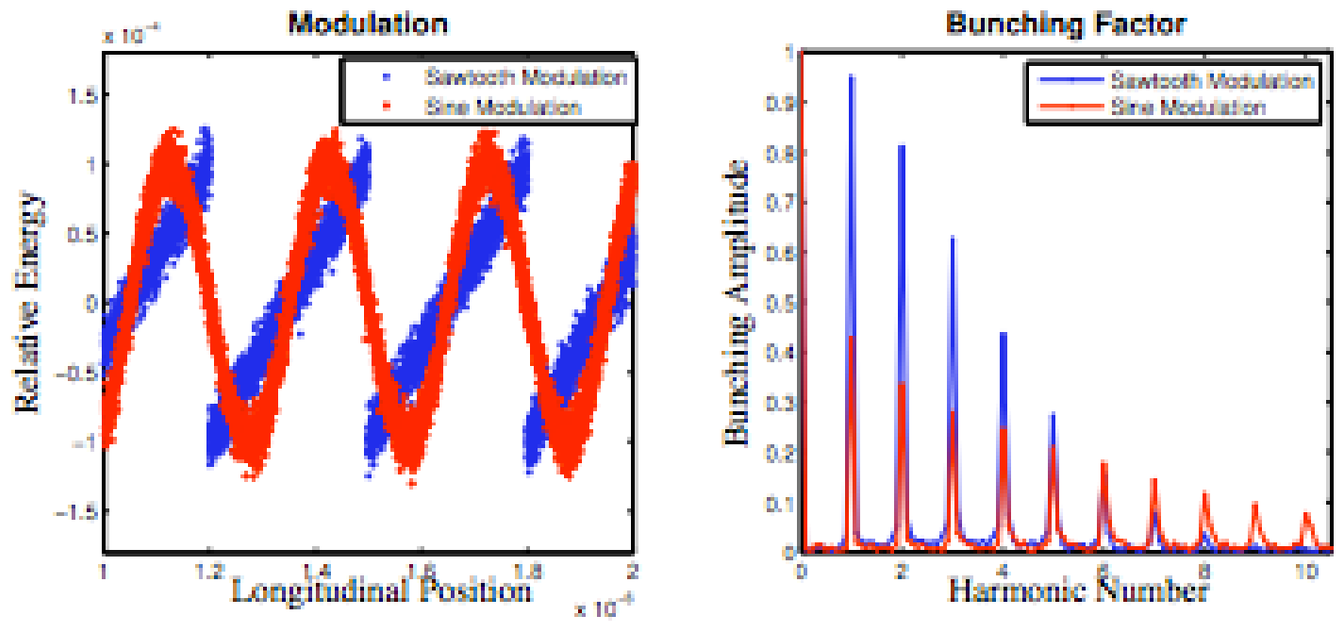

Figure 6: Comparison of equal amplitude sawtooth and sine modulations. The sawtooth increases bunching at low frequencies, but has worse performance at high harmonics.

Figure : from D. Ratner and A. Chao, Proceedings of FEL2011, Shanghai, China

Improving the harmonic bunching with laser harmonics

The linearized portion of the beam allows more electrons to be positioned at specific longitudinal positions after the proper dispersion. This also could improve the performance of EEHG.

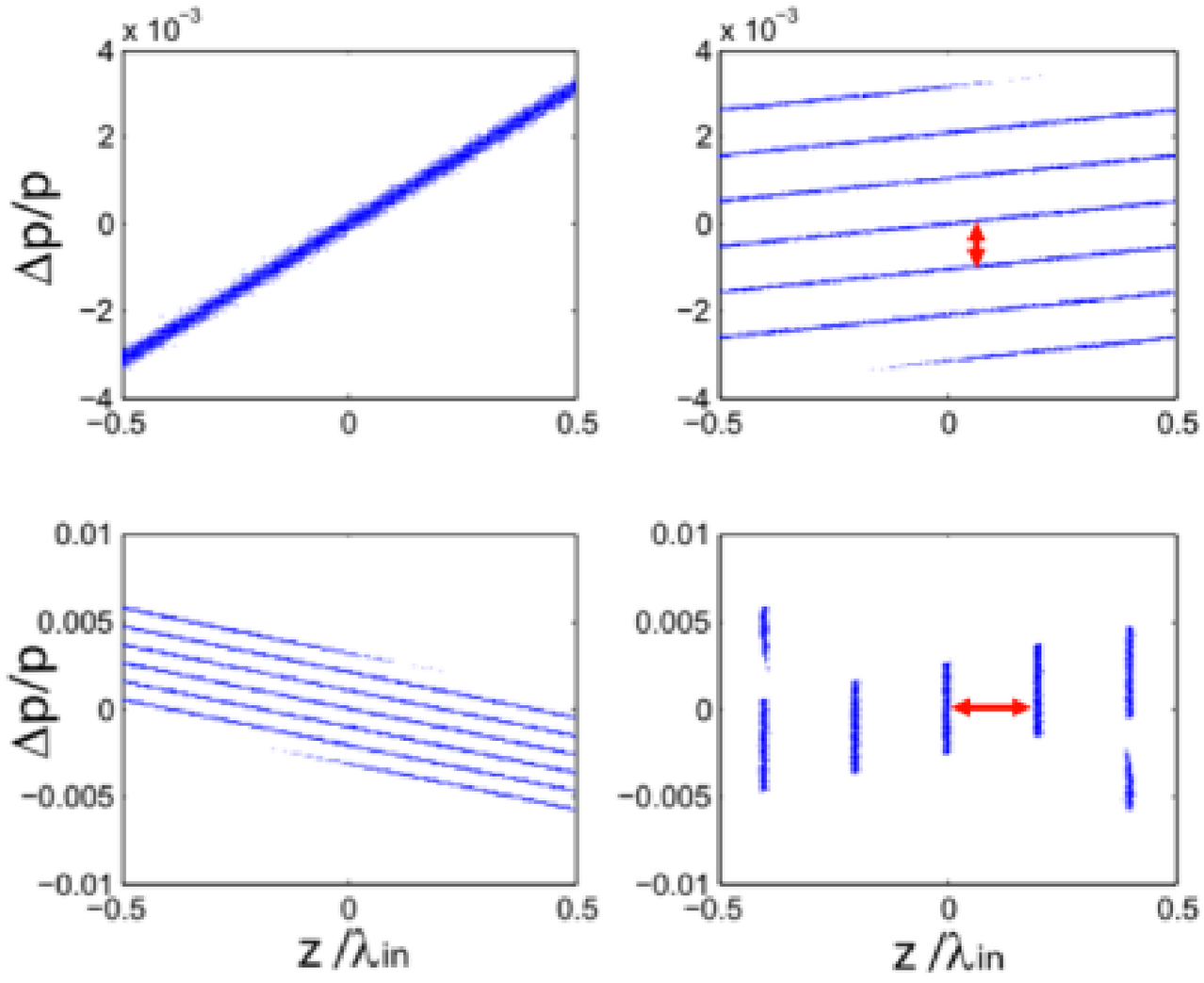

Figure : from D. Ratner and A. Chao, Proceedings of FEL2011, Shanghai, China

Laser based manipulation of beams for free-electron lasers: Short x-ray pulses

Laser slicing

A few-cycle laser pulse can be used to manipulate the beam phase space to select only a short slice for lasing. This technique has another advantage in that the x-ray pulse is naturally synchronized with the laser for pump-probe experiments. One possible implementation of laser based approaches for the generation of attosecond x-ray pulses is shown in Fig. 1.

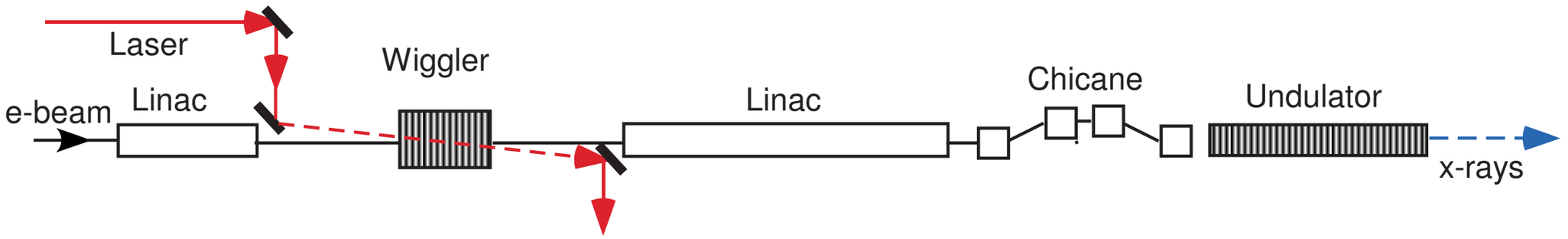

Figure : Schematic of a current enhanced SASE (ESASE) x-ray FEL.

- Bunch is modulated by a short laser pulse that overlaps only a short "working section" (WS) of the beam.

Laser slicing

- Bunch enters a second linac and is accelerated to the final energy (advantageous for tuning and laser power purposes). Phase space frozen.
- Chicane produces bunching in the WS at the laser wavelength and thus a periodic enhancement of the electron peak current.
- Electrons inside the short WS lase from localized current enhancement.

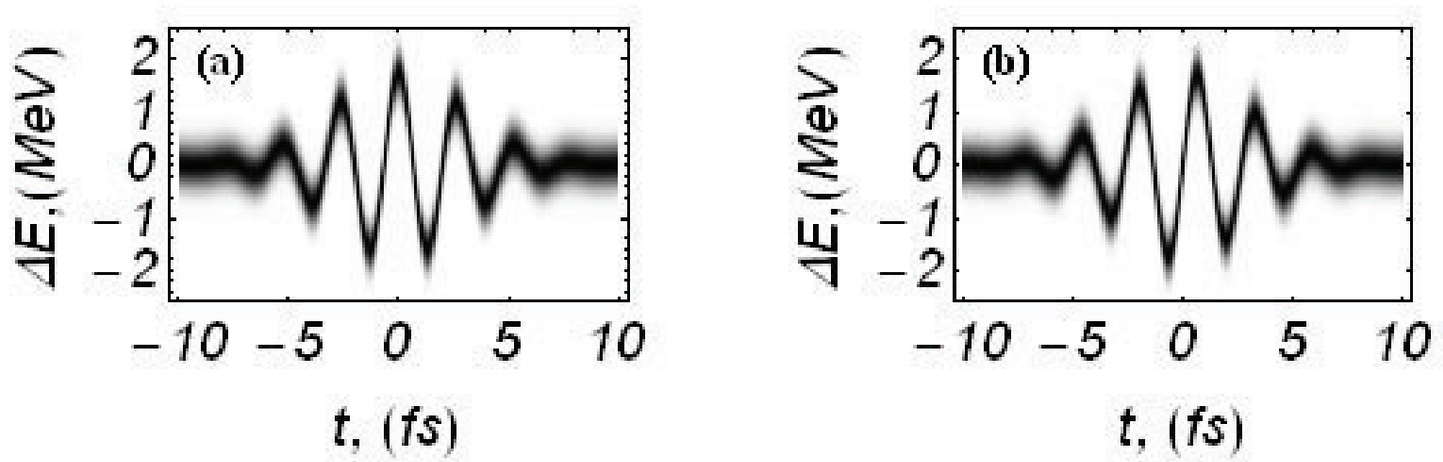

Figure : The phase space of the beam showing energy modulation of electrons produced in the interaction with a few-cycle, 800-nm-wavelength laser pulse with CEP stabilization interacting with the electron bunch in the wiggler magnet with two periods. (a) A cosine-like form, and (b) a sine-like form.

Laser slicing

Besides generating powerful x-rays in the FEL, electrons from the WS can also produce a coherent, temporally synchronized radiation pulse at the modulating laser frequency in a one-period wiggler at the end of the FEL. This signal can be cross-correlated with the laser pulse to provide an accurate measure of the timing jitter between the laser pump pulse and the x-ray probe pulse.

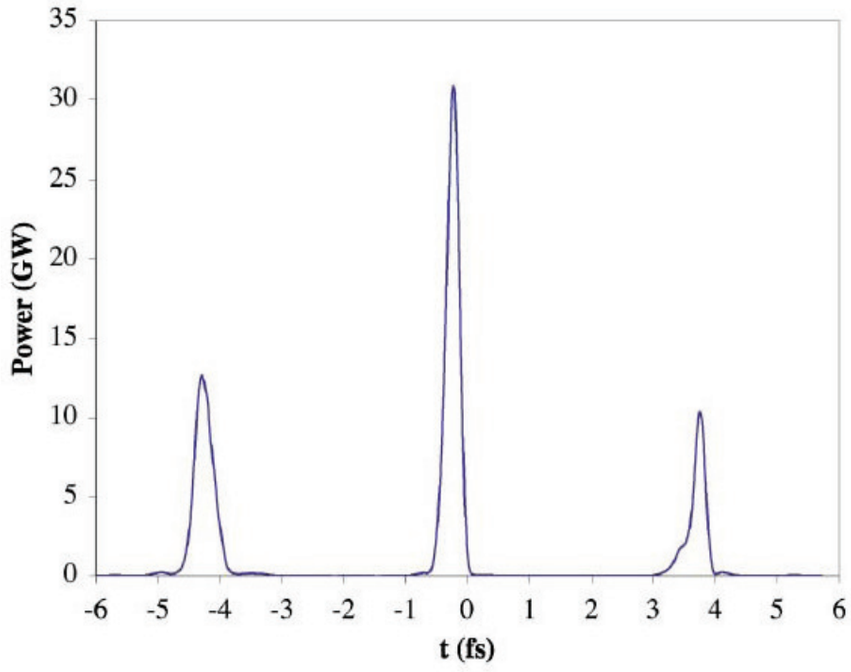

Figure : An example of the x-ray power profile produced in the FEL when using a few-cycle modulating laser. Only a small fragment of the entire x-ray pulse cut at $\pm$ 6 fs is shown. The typical FWHM pulse duration of the central spike is 250 attoseconds.

Laser chirp, undulator taper

Chirp/taper technique: combine undulator tapering with electron beam chirp to enhance FEL output, and make sub-fs x-ray pulses. Recently demonstrated at the SPARC facility at optical wavelengths. Uses a changing K along z to match the local chirp, maintain resonance and extract more power from a selected WS.

$$\frac{d\ln K}{dz} = \frac{\lambda_r}{\lambda_u}\frac{1+K^2/2}{K^2/2}\frac{d\ln\gamma}{ds}. \tag{1.1}$$

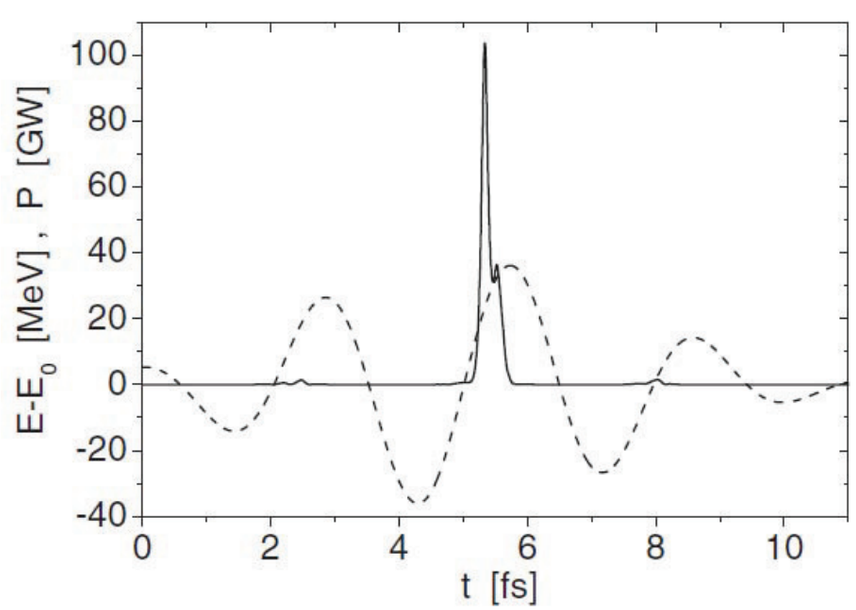

Figure : Energy modulation of the electron beam at the exit of the modulator undulator (dashed line), and a profile of the radiation pulse at the exit of the FEL (solid line).

Laser chirp, undulator taper

Chirp/taper scheme has numerous potential advantages

- Contrast in output can be high because taper only optimized for specific chirp. Gain in unmodulated portions and the modulated regions with the wrong chirp strongly reduced or suppressed, as these electrons fall out of resonance.
- When optimized the calculated x-ray radiation has only one spike about 200 as FWHM.
- Does not require a chicane or density modulation: avoids the potentially strong longitudinal space charge forces that can exist in the ESASE scheme.

Possible disadvantage

- Requires stable interaction between laser and beam to generate reproducible modulation with correct chirp.

Laser chirp, harmonic generation

The preceding laser-based attosecond x-ray pulse generation schemes are all designed for SASE FELs. These require a long undulator which limits the shortest pulse duration to the cooperation length, i.e., ~100 as for hard x-rays with $\AA$ wavelengths, or ~1 fs for soft x-rays with nm wavelengths.

Other methods use lasers or compression to generate a short WS of pre-bunching in the beam to push the pulse length below the cooperation length.

Laser chirp, harmonic generation

A different combination is a variant of EEHG and is also capable of generating ultrashort x-ray pulses with duration well below 100 as.

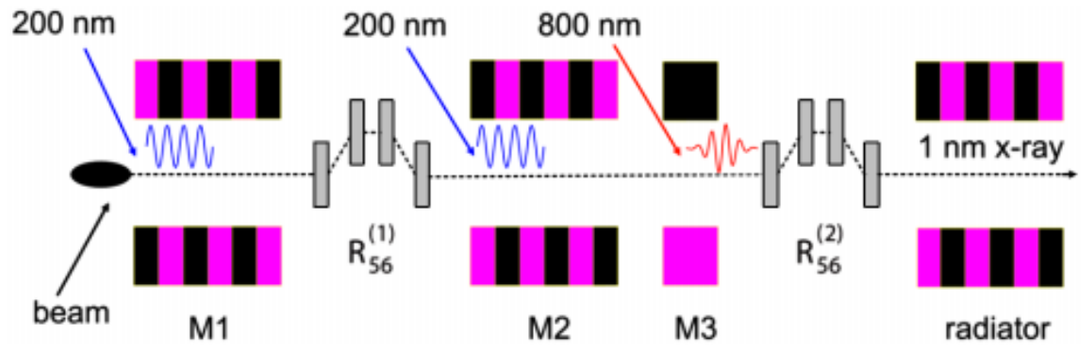

FIG. 1. (Color) Schematic of the proposed scheme for generation of isolated attosecond x-ray pulse.

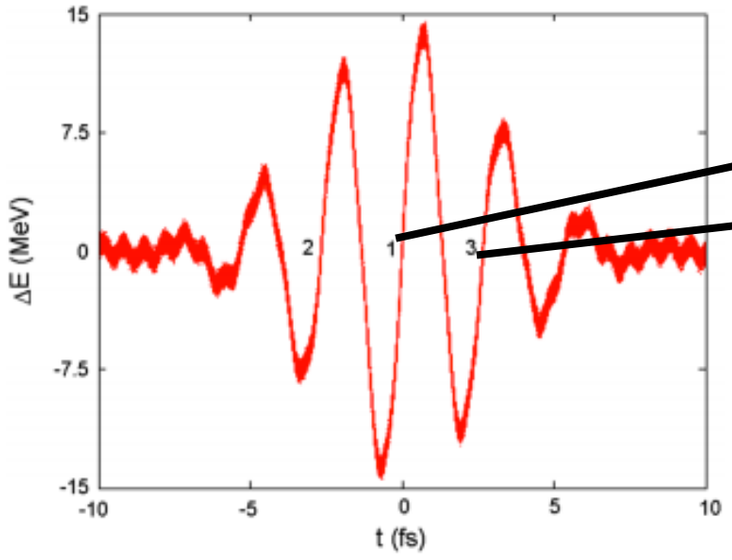

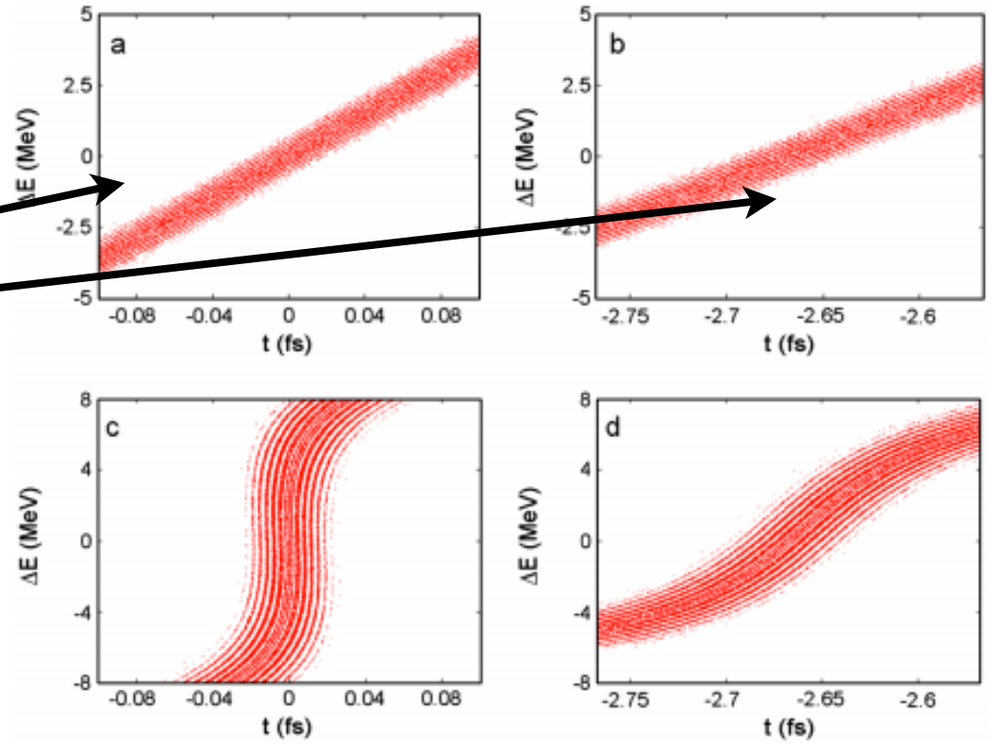

FIG. 5. (Color) Longitudinal phase space of the beam after interaction with the few-cycle laser (bunch head at left).

Multiple pulses, multiple frequencies

Multicolor x-ray FEL pulses

Multicolor x-rays have numerous uses in, e.g., pump-probe experiments. Two of the basic scenarios relevant to two-color x-ray applications are:

- The generation of a pair of sequential x-ray pulses with independent control of timing and spectrum.
- One x-ray pulse with two discrete wavelengths.

Example: Gain Modulated FEL

$$\lambda = \frac{\lambda_u}{2\gamma^2}\left(1 + \frac{K^2}{2}\right)$$

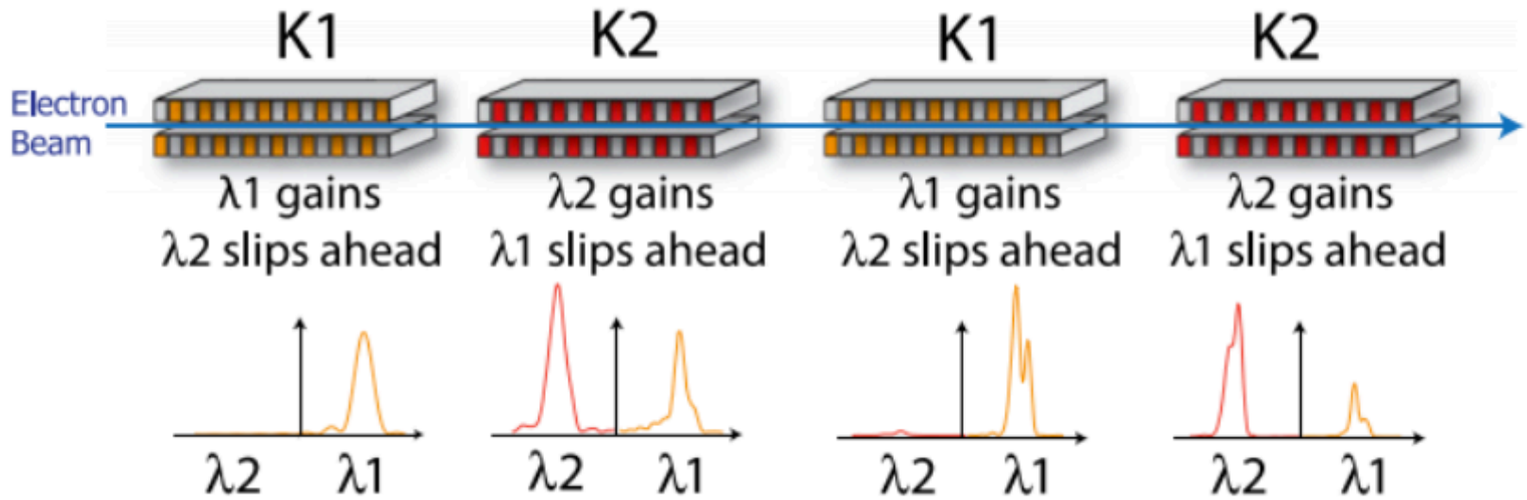

PRL **111,** 134801 (2013) PHYSICAL REVIEW LETTERS week ending 27 SEPTEMBER 2013

Multicolor Operation and Spectral Control in a Gain-Modulated X-Ray Free-Electron Laser

A. Marinelli,[1,*] A. A. Lutman,[1] J. Wu,[1] Y. Ding,[1] J. Krzywinski,[1] H.-D. Nuhn,[1] Y. Feng,[1] R. N. Coffee,[1] and C. Pellegrini[2,1]
[1]*SLAC National Accelerator Laboratory, Menlo Park, California 94025, USA*

Examples: Two or more Color FELs ("Twin beams")

PRL 110, 134801 (2013) PHYSICAL REVIEW LETTERS 29 MARCH 2013

Experimental Demonstration of Femtosecond Two-Color X-Ray Free-Electron Lasers

A. A. Lutman, R. Coffee, Y. Ding,* Z. Huang, J. Krzywinski, T. Maxwell, M. Messerschmidt, and H.-D. Nuhn
SLAC National Accelerator Laboratory, Menlo Park, California 94025, USA
(Received 13 December 2012; published 25 March 2013)

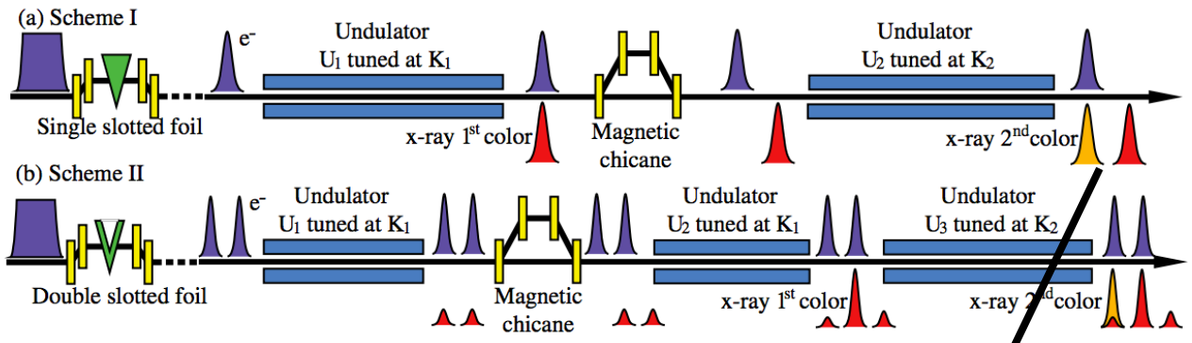

FIG. 1 (color online). Two-color FEL schemes tested at the LCLS. A single-slot (in scheme I) or double-slot (in scheme II) emittance spoiling foil was used to generate ultrashort single or double electron bunches. The emittance-spoiling foil is located in the second bunch compressor. A magnetic chicane, designed for hard x-ray self-seeding purpose, was adopted here to control the temporal delay between the two-color pulses.

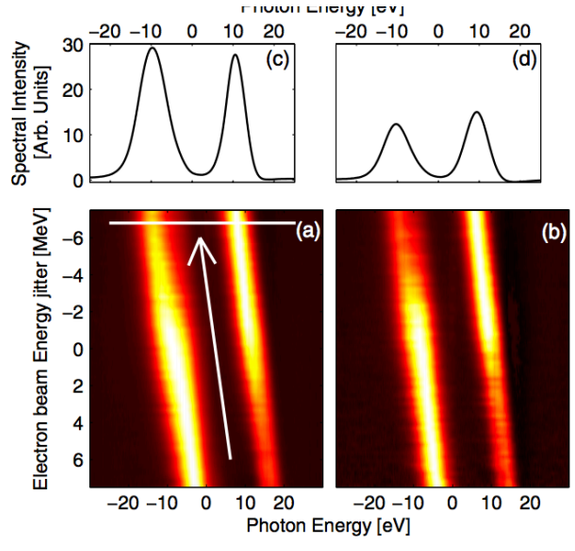

FIG. 3 (color online). Results for two-color beams with scheme I. (a),(b) Average spectral intensity as a function of the electron beam energy and photon energy. For each electron beam energy, the maximum intensity has been normalized to 1. (a) 0 fs delay. (b) 25 fs delay. (c,d) Average realigned spectra as a function of the photon energy offset from 1.5 keV. (c) 0 fs delay. (d) 25 fs delay.

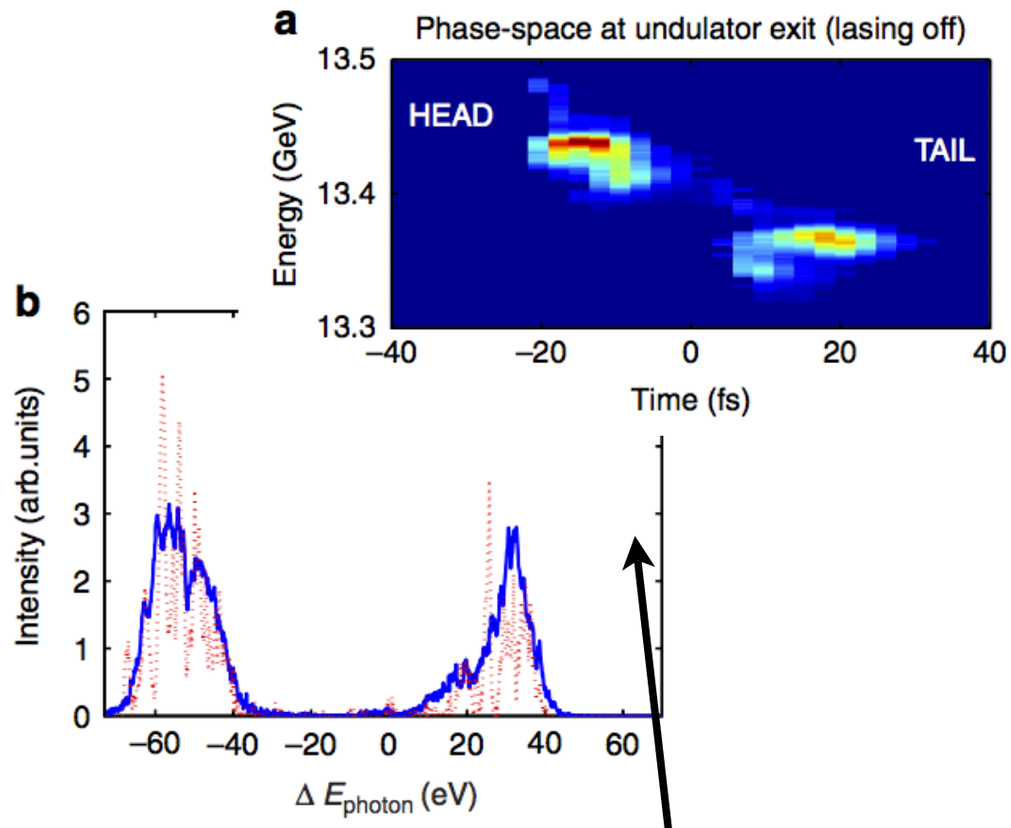

nature COMMUNICATIONS

ARTICLE

Received 16 Oct 2014 | Accepted 22 Jan 2015 | Published 6 Mar 2015

DOI: 10.1038/ncomms7369 OPEN

High-intensity double-pulse X-ray free-electron laser

A. Marinelli[1], D. Ratner[1], A.A. Lutman[1], J. Turner[1], J. Welch[1], F.-J. Decker[1], H. Loos[1], C. Behrens[1,2], S. Gilevich[1], A.A. Miahnahri[1], S. Vetter[1], T.J. Maxwell[1], Y. Ding[1], R. Coffee[1], S. Wakatsuki[1,3] & Z. Huang[1]

Multipulse/multicolor from HGHG FEL

Example: the FERMI FEL. A chirped, high intensity seed laser is used to generate two narrow-band pulses separated both in time and frequency. The bunching factor in FELs seeded by external lasers depends on the energy modulation amplitude. For a laser pulse with a finite length, this amplitude depends on time, so the bunching depends on time. Consider bunching at the 8th harmonic with a time-varying laser pulse amplitude $A(t)$,

$$b_n(t) = e^{-\frac{1}{2}B^2n^2} J_n(-A(t)Bn). \tag{1.4}$$

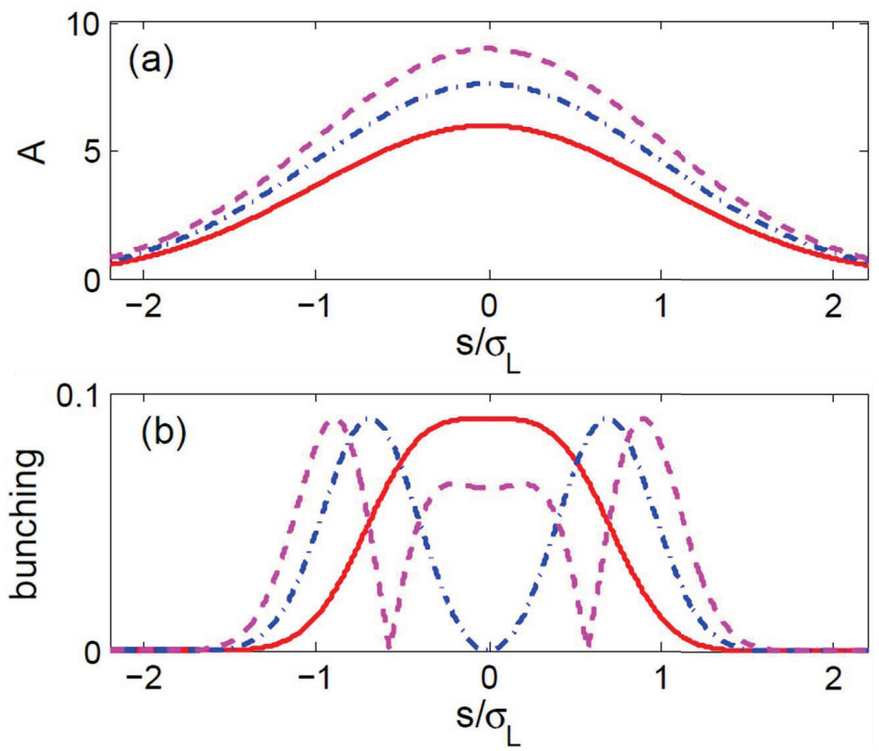

Multipulse/multicolor from HGHG FEL

- For fixed dispersion and small modulation, the bunching distribution has a similar shape as the laser profile, generating a single pulse at a single frequency.
- Larger modulations begin to overbunch the beam, creating a dips in the bunching as dictated by J_n. This beam radiates sequential temporal pulses in the FEL.
- If the laser spectrum is flat, the FEL spectrum shows the interference of the multiple pulses.
- If the laser is chirped, the FEL spectrum has multiple pulses with different frequencies.

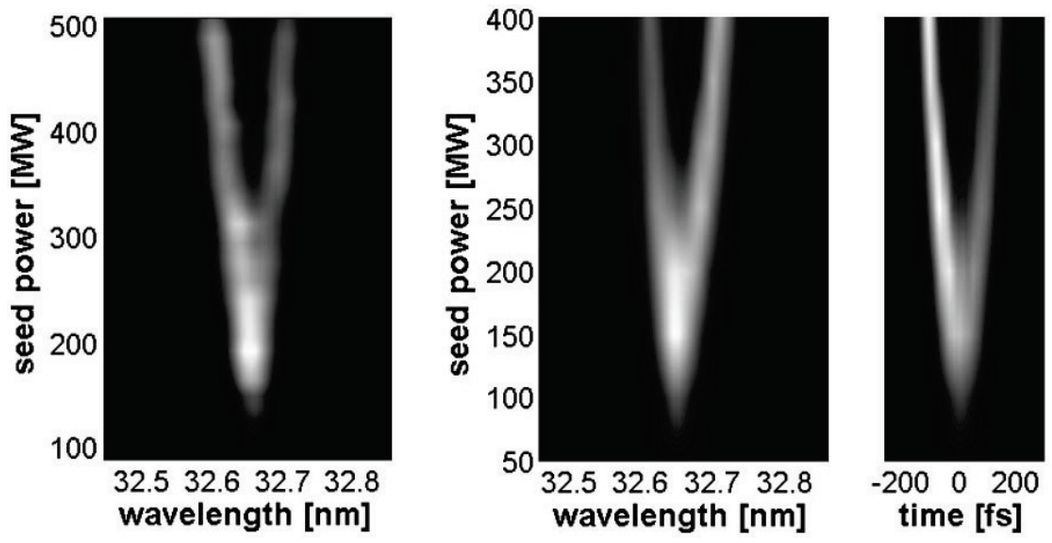

Figure : EUV FEL output for different seed laser powers exp/sim.

Laser driven mode-locked x-ray pulse trains

The preceding techniques are designed to produce a *single* ultrashort x-ray pulse. Here, we discuss another important idea in adapting modern optical techniques to x-rays; namely, the generation of mode-locked x-ray pulses.

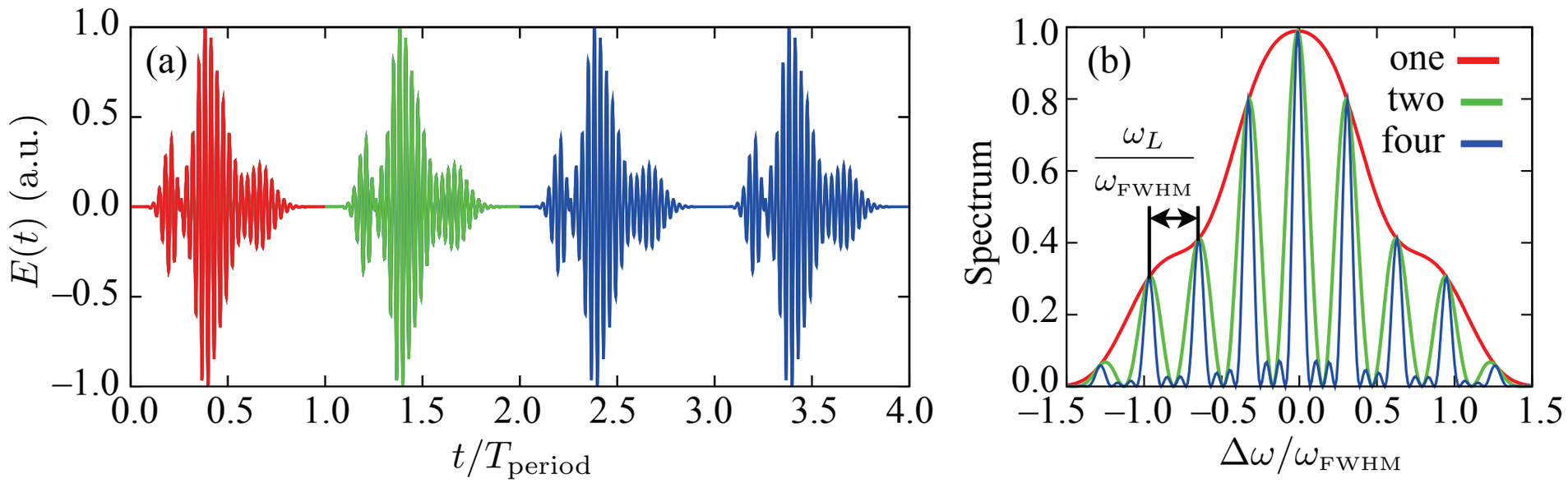

Figure : An example of mode-locking, where the time domain is shown in panel (a) and the frequency domain in panel (b). The single pulse and its spectrum are shown in red. Adding another pulse shown in green in panel (a) leads to the spectrum in panel (b) with additional substructure. The spectrum for the four pulses is shown in blue. (Figure courtesy of R. Lindberg).

Pulse trains

Let us examine a series of N_p light pulses locked in phase. Each pulse has width σ_t, is at the frequency ω_0, and is separated in time by ΔT. The intensity $I(t) \propto |E(t)|^2$ is

$$I(t) \propto \left| e^{i\omega_0 t} \sum_{n=1}^{N_p} e^{-\frac{(t-n\Delta T)^2}{4\sigma_t^2}} \right| \tag{1.2}$$

In the frequency domain $\tilde{E}(\omega) = \int E(t) e^{-i\omega t} dt$, the spectral intensity is

$$\begin{aligned} \tilde{I}(\omega) \propto & e^{2\sigma_t^2(\omega-\omega_0)^2} \left| \sum_{n=1}^{N_p} e^{-in\Delta T(\omega-\omega_0)} \right| \\ = & e^{-2\sigma_t^2(\omega-\omega_0)^2} \frac{\sin^2(\frac{N_p\Delta T}{2}(\omega-\omega_0))}{\sin^2(\frac{\Delta T}{2}(\omega-\omega_0))} \end{aligned} \tag{1.3}$$

Pulse trains

Consider a large number of temporal pulses $N_p \gg 1$. When $\Delta T \gg \sigma_t$, the pulses are well separated in time and there are multiple spikes in the spectrum. These pulses are considered *mode-locked*. There are three scale-lengths of interest:

- The width of the full spectral envelope $\sigma_\omega = 1/2\sigma_t$
- The separation between spectral spikes $\Delta\omega = 2\pi/\Delta T$
- The width of each spectral spike $\delta\omega = 2\pi/N_p\Delta T$

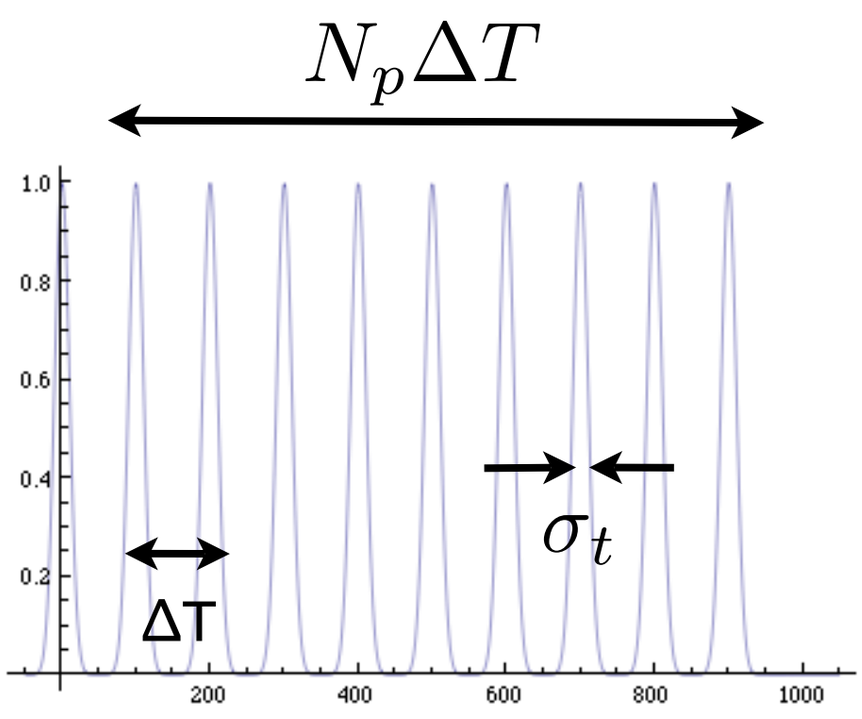

time

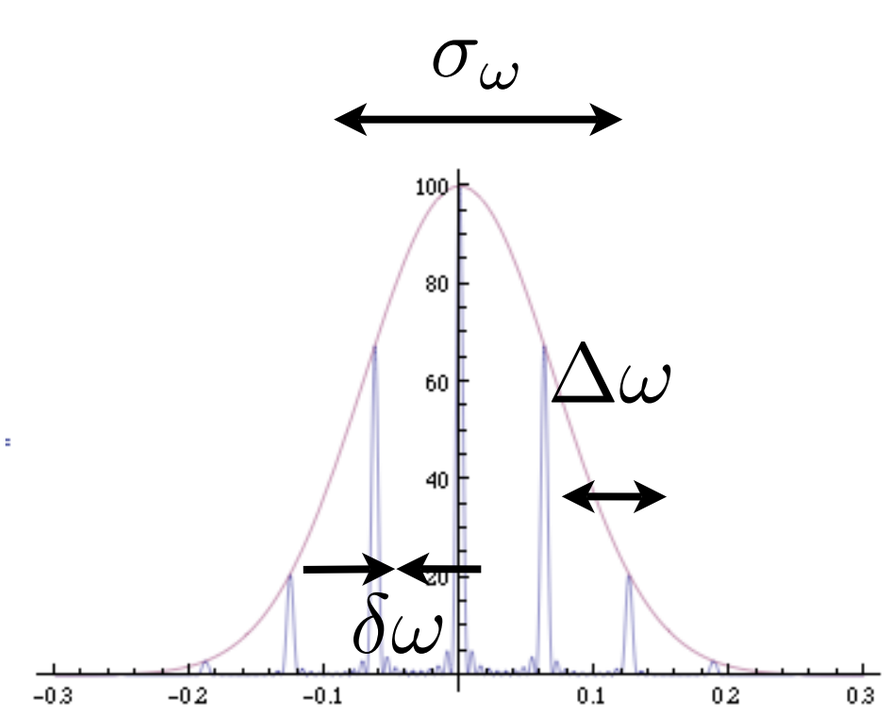

frequency

Pulse trains in high-gain FELs

Mode locking of x-ray pulses in FELs was first introduced in 2008 by Thompson and McNeil. X-ray pulse trains in single pass FELs can be produced by modulating the FEL gain, for example, by modulating the energy of the e-beam in the undulator using an optical laser. Establishing the necessary fixed phase relationship between radiation modes is accomplished by a uniform series of small magnetic chicanes to add precise delays between the e-beam and the radiation field, thereby extending the cooperation length of the FEL radiation.

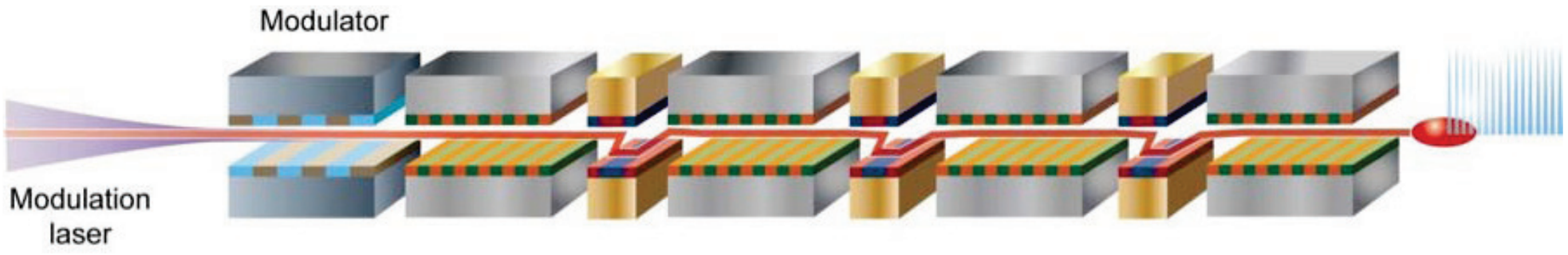

Figure : A schematic of an FEL design with mode-locking capabilities as shown by Thompson and McNeil.

Pulse trains in high-gain FELs

The mode spacing $\Delta\omega = 2\pi/\Delta T$ can be varied by changing the modulating laser wavelength, which requires chicane delay be changed accordingly in order that the total slippage length in each undulator-chicane module is equal to the laser wavelength.
An simulated x-ray signal and spectrum from a mode-locked SASE FEL is shown below. The time domain consists of many ultrashort pulses equally separated by the laser wavelength. The frequency spectrum has many sharp lines over a wide bandwidth. This feature could be beneficial for examining the dynamics of a large number of atomic states simultaneously.

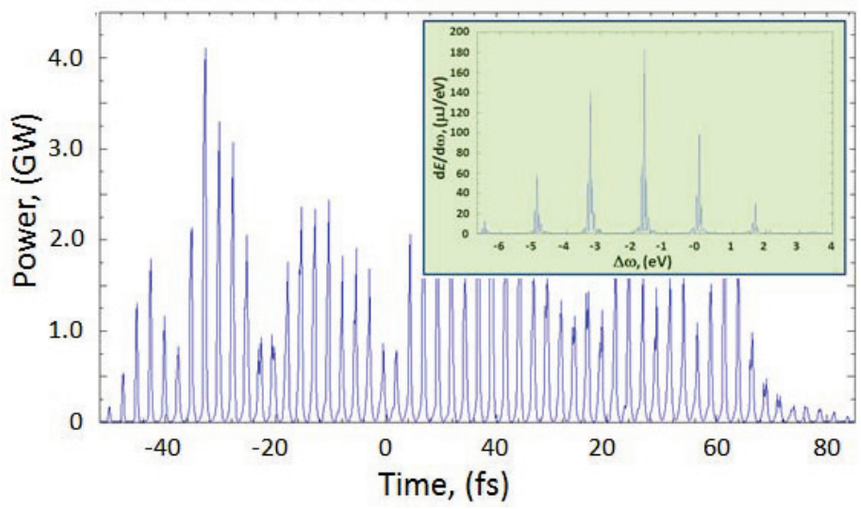

Figure : From Kur 2011.

Summary

- ✦ FELs are highly flexible and versatile!
- ✦ Numerous schemes and techniques exist to tailor or improve the FEL output
- ✦ These days, good ideas can rapidly mature from concept to experiment to implementation
- ✦ Many more good ideas are yet to come...